

Mediterranean Marine Science

Vol 22, No 3 (2021)

VOL 22, No 3 (2021)



Two-way bioinvasion: tracking the neritic non-native cyclopoid copepods *Dioithona oculata* and *Oithona davisae* (Oithonidae) in the Eastern Mediterranean Sea

XIMENA VELASQUEZ, ARSENIY R. MOROV, TUBA TERBIYIK KURT, DALIT MERON, TAMAR GUY-HAIM

doi: [10.12681/mms.26036](https://doi.org/10.12681/mms.26036)

To cite this article:

VELASQUEZ, X., MOROV, A. R., TERBIYIK KURT, T., MERON, D., & GUY-HAIM, T. (2021). Two-way bioinvasion: tracking the neritic non-native cyclopoid copepods *Dioithona oculata* and *Oithona davisae* (Oithonidae) in the Eastern Mediterranean Sea. *Mediterranean Marine Science*, 22(3), 586–602. <https://doi.org/10.12681/mms.26036>

Two-way bioinvasion: tracking the neritic non-native cyclopoid copepods *Dioithona oculata* and *Oithona davisae* (Oithonidae) in the Eastern Mediterranean Sea

Ximena VELASQUEZ^{1,2}, Arseniy R. MOROV¹, Tuba TERBIYIK KURT³, Dalit MERON^{2,4,5}
and Tamar GUY-HAIM^{1,5}

¹ Biology Department, National Institute of Oceanography, Israel Oceanographic and Limnological Research (IOLR), Haifa, Israel

² Department of Marine Biology, Leon H. Charney School of Marine Sciences, University of Haifa, Israel

³ Department of Marine Biology, Faculty of Fisheries, Cukurova University, Adana, Turkey

⁴ Morris Kahn Marine Research Station, University of Haifa, Israel

⁵ Hong Kong Branch of Southern Marine Science and Engineering Guangdong Laboratory (Guangzhou), Hong Kong, China

Corresponding author: tamar.guy-haim@ocean.org.il

Contributing Editor: Maria MAZZOCCHI

Received: 4 February 2021; Accepted: 22 August 2021; Published online: 14 October 2021

Abstract

Accelerated anthropogenic changes in the Eastern Mediterranean Sea (EMS) have facilitated the introduction, spread and establishment of invasive copepod species in this region. Here, we report for the first time the introduction of two non-native cyclopoid copepods *Dioithona oculata* and *Oithona davisae* in Israeli coastal waters and describe their temporal variability. The species were identified based on morphological characteristics, DNA barcoding, and phylogenetic inference. Molecular identification and phylogenetic analysis supported the taxonomic identification, but showed cryptic speciation within *D. oculata*, separating the Western Pacific and EMS clades. In Israeli coastal waters, *D. oculata* exhibited a temporally restricted occurrence, appearing from September to December 2019 and in October 2020. *D. oculata* peaked in autumn, when seawater temperature was 28 °C. Its lowest abundance was observed in December when temperature decreased to 21 °C, indicating that the thermal affinity of *D. oculata* for warm-temperate conditions, for reproduction and the maintenance of viable populations, persisted in the introduced range. In contrast, *O. davisae* appeared almost year-round. It peaked at a summer temperature of 28 °C, as well as under the winter minimum of 17 °C, confirming its wide eurythermal tolerance. Based on our findings and previous observations, we suggest that *D. oculata* may have invaded the EMS through the Suez Canal and is now at the onset of its spread in the Mediterranean Sea, whereas *O. davisae* has been introduced via shipping, likely from the Northeast Atlantic, widely spreading and successfully establishing viable populations throughout the entire Mediterranean Sea to the coastal Levantine Sea.

Keywords: Oithonidae; Levantine Basin; tropicalization; bioinvasion vectors; DNA barcoding; Mt-COI gene.

Introduction

The Mediterranean Sea coastal waters have become an ideal environment for biological invasions due to the tropicalization of the region by the prolonged warming over the past several decades (Bianchi & Morri, 2003), which has facilitated numerous introductions of non-native species with thermophilic affinity from warmer regions such as the Indo-Pacific province and the subtropical-equatorial Atlantic Ocean (Mannino *et al.*, 2017). Most non-native copepods in the Mediterranean Sea coastal waters are of Indo-Pacific origin, and were first introduced into the Levantine Basin via the Suez Canal and by ballast water from shipping and hull fouling (Katsanevakis *et al.*, 2014; Armon & Zenetos, 2015; Sabia *et al.*, 2015). To date, 61 non-native copepods have been recorded in the

Mediterranean Sea, of which 12 are cyclopoid copepods (based on a compilation of Abdel-Rahman, 2005; Zenetos *et al.*, 2010, 2012, 2020; Zakaria, 2015).

Cyclopoid species are the most abundant small-sized copepods within mesozooplankton communities, playing an essential role in pelagic food webs, microbial loop, and carbon cycling (Turner, 2004; Zervoudaki *et al.*, 2007). Oithonidae is the most dominant family of cyclopoid copepods in terms of diversity, abundance, and productivity in coastal marine environments (Castellani *et al.*, 2007; Hwang *et al.*, 2010). These cyclopoids occur at high densities in the epipelagic and mesopelagic zones, substantially contributing to the overall mesozooplankton abundance in temperate regions such as the Mediterranean Sea.

Oithonidae includes species with differential levels of

adaptability to environments with different physicochemical properties, displaying both worldwide and narrower ranges of distribution (Dahms *et al.*, 2015). *Dioithona oculata* (Farran, 1913) is an example of an oithonid that exhibits a wide distribution range. This tropical species has been recorded in several regions (Fig. 1), mostly in the Caribbean Sea, Western Pacific and Indian Ocean (Razouls *et al.*, 2005-2021). Recently, *D. oculata* was reported for the first time as an alien species in the northeastern Mediterranean Sea (Terbiyik Kurt, 2018). The native range of *D. oculata* comprises mainly mangrove swamps, coastal lagoons, estuaries and reefs. In these habitats, it forms dense swarms of adult individuals as a strategy for protection from fish predation and to increase mating and reproductive success (Hammer & Carleton, 1979; Ambler *et al.*, 1991; Buskey, 1998; Hsiao *et al.*, 2013). In its invaded distribution range, *D. oculata* has been found in coastal water environments (Terbiyik Kurt, 2018, 2020a).

In its native range, *Oithona davisae* (Ferrari & Orsi, 1984) inhabits the temperate coastal waters of East Asia, including the Sea of Japan and the South China Sea (Nishida, 1985; Razouls *et al.*, 2005-2021, Fig. 1). However, over the past 50 years, this species has expanded its distribution (Table 1) to the North and South Pacific Ocean (Ferrari & Orsi, 1984; Hirakawa, 1988), the North Atlantic Ocean (Cornils & Wend-Heckmann, 2015; Uriarte *et al.*, 2016), the Black Sea (Zagorodnyaya, 2002), and the Mediterranean Sea (Saiz *et al.*, 2003), where it has successfully spread and established viable populations across the western, central and eastern basins (Zagami *et al.*, 2018; Terbiyik Kurt & Beşiktepe, 2019; Pansera *et al.*, 2021, Fig. 1). *O. davisae* is very abundant in eutrophic waters within its native range (Uye & Sano, 1995; 1998), but it has also been shown to have high adaptability to a wide range of haline and thermal conditions, and can survive and reproduce in various non-native coastal habitats (Svetlichny & Hubareva, 2014; Cornils & Wend-Heckmann, 2015; Svetlichny *et al.*, 2016).

Here, we report for the first time, the introduction of *D. oculata* and *O. davisae* in Israeli coastal waters. Our findings are supported by the morphological identification of the two species, which was confirmed by DNA barcoding and phylogenetic inference. Moreover, we present the temporal distribution of their abundances during a one-year investigation in two different coastal habitats, and we discuss the potential introduction and dispersal vectors that may facilitate their spread and establishment in the Eastern Mediterranean Sea (EMS).

Material and Methods

Zooplankton sample collection

Mesozooplankton samples were collected monthly by horizontal net tows (65 and 200 µm mesh size, Sea-Gear, USA), at a depth of 0.5-1 m for 20 min each, in nearshore coastal waters (bottom depth 15-30 m) near Hadera, Israel (32.4700° N, 34.6930° E) between September 2019 and October 2020. Additional samples were collected at the Qishon Harbour (32.8062° N, 35.0305° E) using horizontal tows for 10 min (bottom depth 6-11 m) in October 2020 (Fig. 2). The nets were equipped with a mechanical flow meter (Sea-Gear, USA) to standardize the samples per filtered water volume. The samples were kept on ice, transported within 1 h to the laboratory, and halved using a plankton sample splitting box (Motoda, 1959) at the Israel Oceanographic and Limnological Research (IOLR). One-half of the sample was fixed with buffered 4% formalin solution for morphological examination and species quantification, while the other half was preserved in 96% ethanol (*D. oculata* specimens) or at -20 °C (*O. davisae* specimens) for molecular identification. Additionally, 96% ethanol-preserved specimens of *D. oculata* (İskenderun Bay, 36.8190° N, 35.9327° E) and *O. davisae* (İzmir Inner Bay, 27.0567° N, 38.4307° E) from

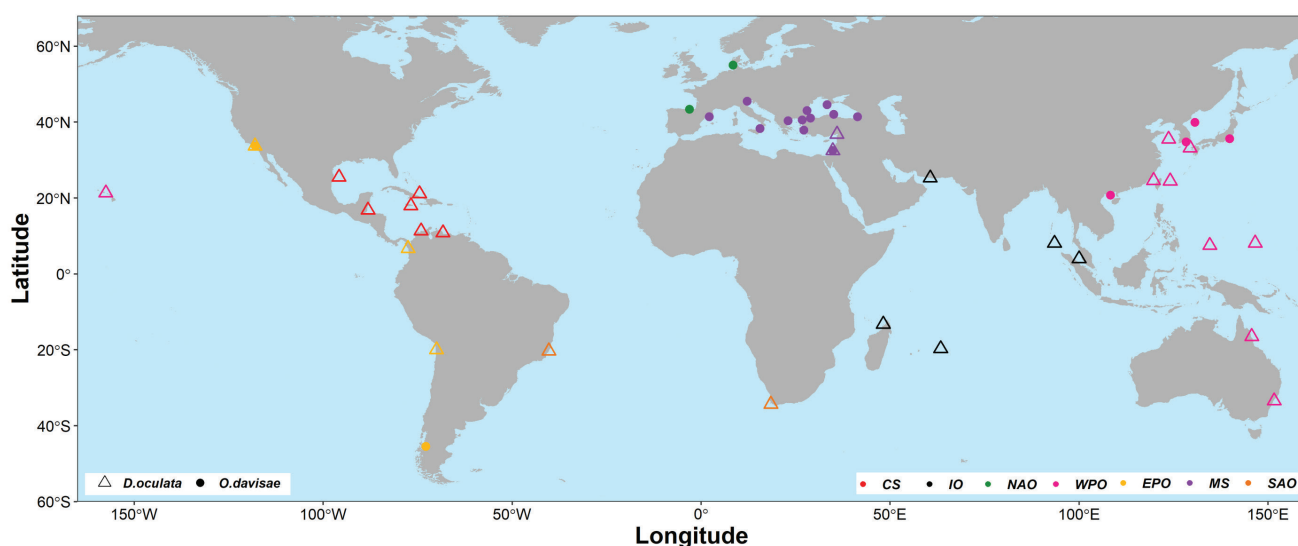


Fig. 1: Worldwide distribution of *Dioithona oculata* and *Oithona davisae*, showing species distribution across native and invaded ranges. Colours indicate regions and shapes indicate species. CS: Caribbean Sea, MS: Mediterranean Sea, EPO: Eastern Pacific Ocean, IO: Indian Ocean, SAO: South Atlantic Ocean, WPO: Western Pacific Ocean. *D. oculata* (Farran, 1913) and *O. davisae* (Ferrari & Orsi, 1984) in GBIF Secretariat (2020). GBIF Backbone Taxonomy. Checklist dataset <https://doi.org/10.15468/39omei>.

Table 1. Locations and years of first records of *Oithona davisae*.

| Invaded region, Country | Year | Reference |
|--|---|--|
| Eastern Pacific Ocean | | |
| San Francisco Bay, USA | prior to 1966 | Ferrari & Orsi (1984) |
| Chile | 1980-1986 | Hirakawa (1988) |
| Atlantic Ocean (North Sea) | | |
| Northern Wadden Sea, Germany | 2010 | Cornils & Wend-Heckmann (2015) |
| Bay of Biscay, France | 2001 | Uriarte <i>et al.</i> , (2016) |
| Mediterranean Sea | | |
| Western basin | | |
| Barcelona Port, Spain | 2000 | Saiz <i>et al.</i> , (2003) |
| Central basin | | |
| Lakes Faro and Ganzirri, Italy | 2014 | Zagami <i>et al.</i> , (2018) |
| Adriatic Sea | | |
| Venice, Italy | 2014-2015 | Vidjak <i>et al.</i> , (2019) |
| Venice Lagoon, Italy | 2016-2017 | Pansera <i>et al.</i> , (2021) |
| Black Sea | | |
| Sevastopol Bay, Ukraine | 2001 (identify as <i>Oithona brevicornis</i>), 2005-2006 2008, 2010 (re-examination and identification as <i>Oithona davisae</i>) 2005-2009 | Zagorodnyaya (2002), Gubanova & Altukhov (2007) Temnykh and Nishida (2012) Altukhov <i>et al.</i> , (2014) |
| Novorossiysk, Tuapse, Gelendzhik, And Anapa, Northeastern part, Russia | 2004-2007 identify as <i>Oithona brevicornis</i>) | Selifonova (2009) |
| Varna and Bourgas Bays, Cape Kaliakra, Western part, Bulgaria | 2009-2012 2013 | Mihneva & Stefanova (2013) Shiganova <i>et al.</i> , (2015) |
| Turkish coast of Black Sea, Sinop coast | 2009 | Üstün & Terbiyik Kurt (2016) |
| Sürmene Bay, Turkey | 2010-2014 | Yıldız <i>et al.</i> , (2017) |
| Marmara Sea | | |
| Büyükçekmece Bay, Turkey | 2014 | Doğan & Isinibilir (2016) |
| Golden Horn Estuary, Turkey | 2015 | Isinibilir & Doğan (2019) |
| Aegean Sea | | |
| Thermaikos Bay, Greece | 2018 | Dragicevic <i>et al.</i> , (2019) |
| Turkey Coast | 2015 | Terbiyik Kurt & Besiktepe, 2019 |
| Levantine Basin | | |
| İskenderun Bay, Turkey | 2018 | Terbiyik Kurt (2020b, Personal Communication) |
| Hadera and Qishon harbour, Israel | 2019, 2020 | This study |

Turkey were included in this study for molecular identification and comparison with Israeli specimens.

Environmental variables

Seawater temperature, salinity and fluorescence (calibrated and converted to chlorophyll *a*, µg L⁻¹) were measured continuously at the Hadera site using a stationary CTD (SBE 19PlusV2, SeaBird, USA) with a high-resolution fluorometer (WET Labs ECO, SeaBird, USA) fixed at 13 m depth since 2003 for the National Monitoring Program of the Israeli Mediterranean Sea (the data are available online at <https://isramar.ocean.org.il>,

at the Israel Marine Data Center). The temperature and salinity in Qishon Harbour were measured during mesozooplankton sampling using a non-fixed CTD (Sea-Bird SBE 19PlusV2, USA). Seawater samples were collected for flow cytometry analyses to determine the abundance of pico- and nano-eukaryotes (cells/µL). Samples (1.7 mL) were fixed with flow-cytometry-grade glutaraldehyde (0.02% final concentration, G7651, Sigma-Aldrich, USA), frozen in liquid nitrogen, and stored at -80 °C until analysis. Taxonomic discrimination was based on the orange fluorescence of phycoerythrin (585 nm), red fluorescence of chlorophyll *a* (630 nm), side-scatter (SSC, a proxy of cell volume), and forward-scatter (FSC, a proxy of cell size) (Raveh *et al.*, 2015).

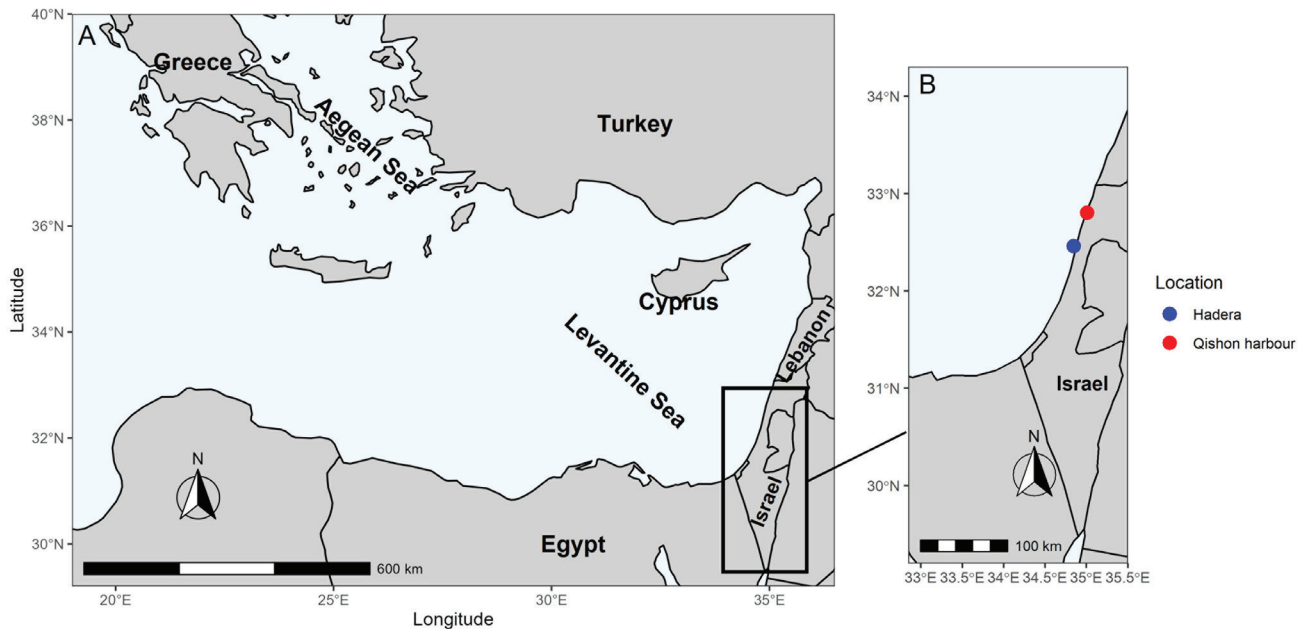


Fig. 2: Map showing the sampling region. A) General view of the Eastern Mediterranean Sea. B) The Israeli coast at the southeast Levantine Sea, indicating the sampling sites: Hadera and Qishon Harbour.

Morphological identification

D. oculata and *O. davisae* specimens were examined under a stereomicroscope (Olympus SZX16, Olympus, Japan) and a light microscope (Olympus BX50, Olympus, Japan). Morphological measurements such as prosome length, (PL), urosome length (UL), caudal ramus length (CRL), caudal ramus width (CRW), total length (PL+ UL +CRL, measured dorsally) P:U ratio and CRL:CRW ratio, were taken from ten male and ten female individuals of *D. oculata* and ten female individuals of *O. davisae*, collected in October 2019 at the Hadera site (Table 2). The specimens were dissected to obtain mouthparts and swimming legs and the taxonomic identifications followed the classification system proposed by Bradford-Grieve *et al.* (1999), Razouls *et al.* (2005-2021), and the taxonomic description made by Terbiyik Kurt (2018) for *D. oculata*, and Ferrari & Orsi (1984) for *O. davisae*. Additionally, six female and six male specimens of *D. oculata* (fixed in 4% formalin, in 1.7 mL vials) and four females of *O. davisae* from Hadera and Qis-

hon Harbour (collected in October 2020) were deposited in the National Natural History Collections of the Hebrew University in Jerusalem and assigned the following voucher numbers: HUJIKINOR6000-HUJIKINOR6003; HUJIKINOR6006-HUJIKINOR6007 and HUJIKINOR6004-HUJIKINOR6005; HUJIKINOR6008-HUJIKINOR6009, respectively.

Species abundance and temporal variation

For each monthly sample, one to five subsamples were taken with a calibrated Plunger Hensen-pipette (2.5 mL; Hydro-Bios, Germany) and counted using a Bogorov chamber. A minimum of 30 *D. oculata* and 20 *O. davisae* individuals were counted per each subsample. Abundances (ind. m⁻³) of adult individuals (males and females) and copepodites (stage was not distinguished) were calculated in samples collected with the 200 µm plankton net for *D. oculata* and in samples collected with the 65 µm net for *O. davisae* (only adult females) due to their

Table 2. Morphological measurements of *Dioithona oculata* and *Oithona davisae* specimens collected in October 2019 at the Hadera site. Mean and standard deviation of the prosome length, (PL), urosome length (UL), caudal ramus length (CRL), caudal ramus width (CRW), total length (PL+ UL +CRL, measured dorsally) P: U ratio and CRL: CRW ratio.

| Species | PL (µm) | UL (µm) | CL (µm) | Total length (µm) | CRW (µm) | L:W | P:U |
|---------------------------|---------|---------|---------|-------------------|----------|---------|---------|
| <i>D. oculata</i> -female | 431±32 | 267±12 | 33±3 | 731±44 | 14±1.2 | 2.1-2.5 | 1.4-1.7 |
| <i>D. oculata</i> -male | 413±26 | 239±24 | 31±1 | 683±50 | 13±0.7 | 2.2-2.5 | 1.6-1.9 |
| <i>O. davisae</i> -female | 314±13 | 210±18 | 28±4 | 552±33 | 9±0.9 | 2.7-3.2 | 1.4-1.6 |

smaller size (Riccardi, 2010). The relationships between the abundances of the two species and environmental parameters were determined by Spearman correlation using the “Vegan” package in R (Oksanen *et al.*, 2013).

Molecular identification

Total DNA was extracted from the ethanol-preserved specimens of *D. oculata* and *O. davisae* (1–5 individuals were pooled) and the preserved frozen specimens of *O. davisae* (per each individual separately) using the DNEasy Blood and Tissue kit (QIAGEN, Germany) according to the manufacturer’s specifications. The mitochondrial cytochrome *c* oxidase subunit I (*COI*) gene was amplified using the two primer pairs Cop-COI-1498F (5’-AAYCATAAAGAYATYGGDAC-3’)/ HCO2198R (5’-TAAACTTCAGGGTGACCAAAAAATCA-3’) for *D. oculata* and LCO1490F (5’-GGTCAACAAATCATAAAGATATTGG-3’)/Cop-COI-2189R (5’-GGGTGACCAAAAAATCARAA-3’) for *O. davisae* (Bucklin *et al.*, 2010). PCR conditions were as follows: 95°C for 5 min, 40 cycles of 95°C for 1 min, 45°C for 1 min, 72°C for 1 min, and a final cycle of 72°C for 7 min. The PCR products were purified and sequenced by Hy Laboratories Ltd. (Israel).

The obtained sequences were edited and corrected using BioEdit (Hall, 1999) and deposited in GenBank (<https://www.ncbi.nlm.nih.gov/>). The NCBI accession numbers are shown in Table 3. To identify *D. oculata* and *O. davisae* at the species level, the sequences were compared with the NCBI database using blastn (<https://blast.ncbi.nlm.nih.gov/>). *COI* sequences of different *D. oculata* and *O. davisae* specimens from other regions were

downloaded from GenBank and aligned using ClustalW in MEGA-X (Kumar *et al.*, 2018). Evolutionary models and parameter estimates were selected using the lowest AICc score obtained with ModelTest to create a phylogenetic and molecular evolutionary analysis, using a Maximum Likelihood method. The phylogenetic tree based on the *COI* sequences was generated using the best-fitting model Hasegawa-Kishino Yano (HKY)+I. The tree was run with 1000 bootstrap replicates. Additionally, genetic distances (p-distances) were calculated using a pairwise distance matrix.

Results

Morphology of *Dioithona oculata*

The mean total body length (TL) of the females was $730 \pm 5 \mu\text{m}$ (n=10) while males were smaller in size with a TL of $680 \pm 5 \mu\text{m}$ (n=10). The female prosome is oval and robust with a rounded anterior part (Fig. 3A), while the male prosome is elongated with a square-like anterior part (Fig. 4A), similar to the specimens described by Terbiyik Kurt (2018) from Turkish coastal waters. In both sexes, the rostrum is blunt, and two distinct big eye lenses are visible (Figs. 3A, 3B, 4A, 3B). The eyes lenses present blue pigmentation in the formalin-fixed specimens as described by Terbiyik Kurt (2018), while in live specimens, the lenses are black (Supplementary material Video S1, on line). The female and male urosomes contain orange pigmentation (Figs. 3A, 4A), which was observed in the specimens described by Terbiyik Kurt (2018), but not mentioned in the original description by Farran (1913). The following morphological characteristics are common

Table 3. *Dioithona oculata* and *Oithona davisae* *COI* sequences (GenBank) used for the molecular identification, phylogenetic analysis and pairwise distance matrix. * denote sequences used from BOLD Systems. AgS: Aegean Sea, EMS: Eastern Mediterranean Sea, EPO: Eastern Pacific Ocean; NAS: North Atlantic Ocean, WPO: Western Pacific Ocean.

| Species | Place of collection | Accession Numbers | References |
|--|-------------------------------|--|--------------------------------|
| <i>Dioithona oculata</i> | Hadera, Israel (EMS) | MW309846, MW309848, MW309850, MW309852, MW309854 | This study |
| <i>Dioithona oculata</i> | Iskendrun Bay, Turkey (EMS) | MW309856, MW309858, MW309860 | This study |
| <i>Dioithona oculata</i> | Kaneohe Bay, Hawaii (WPO) | KC594141.1- KC594144.1 | Jungbluth & Lenz (2013) |
| <i>Oithona davisae</i> | Hadera, Israel (EMS) | MW535673- MW535677 | This study |
| <i>Oithona davisae</i> | Izmir inner bay, Turkey (AgS) | MZ618916, MZ618918, MZ618920 | This study |
| <i>Oithona davisae</i> | Northern Wadden Sea (NAS) | KP033179.1- KP033188.1 | Cornils & Wend-Heckmann (2015) |
| <i>Oithona davisae</i> | California, USA (EPO) | ZPC080-13.COI-5P*, ZPC208-14.COI-5P* | BOLD Systems |
| <i>Paracyclops chiltoni</i> (Outgroup) | Yucatan Peninsula, Mexico | MK370314.1 | Khodami <i>et al.</i> , (2019) |

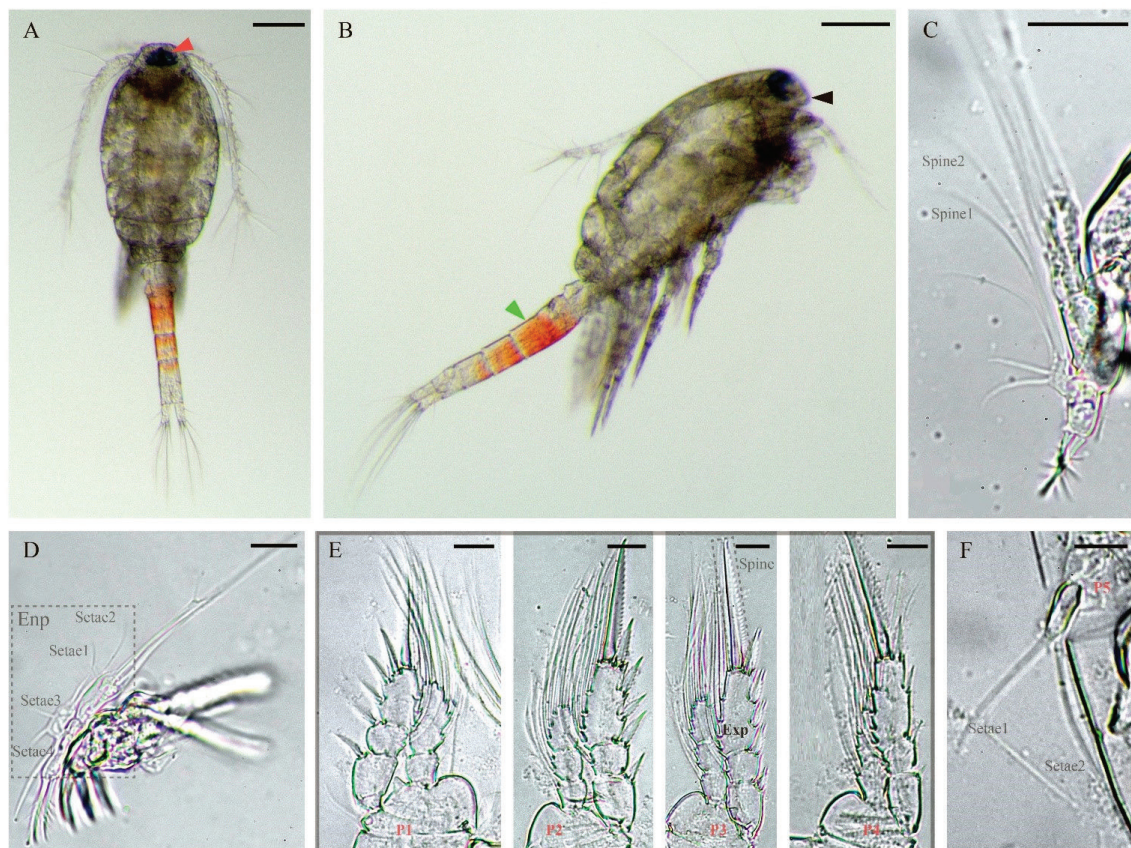


Fig. 3: Main morphological characteristics of *Dioithona oculata*, fixed female specimens. A) Dorsal view (red arrowhead depicts big eye lens with blue pigmentation). B) Lateral view (black arrowhead depicts blunt rostrum, green arrowhead depicts genital somite in the urosome). C) Mandible. D) Maxillule. E) P1 - P4 swimming legs. F) P5 leg. Enp - endopod; Exp - exopod. Scale bars for A, B - 100 μ m; for C, D, E - 20 μ m; for F - 10 μ m.

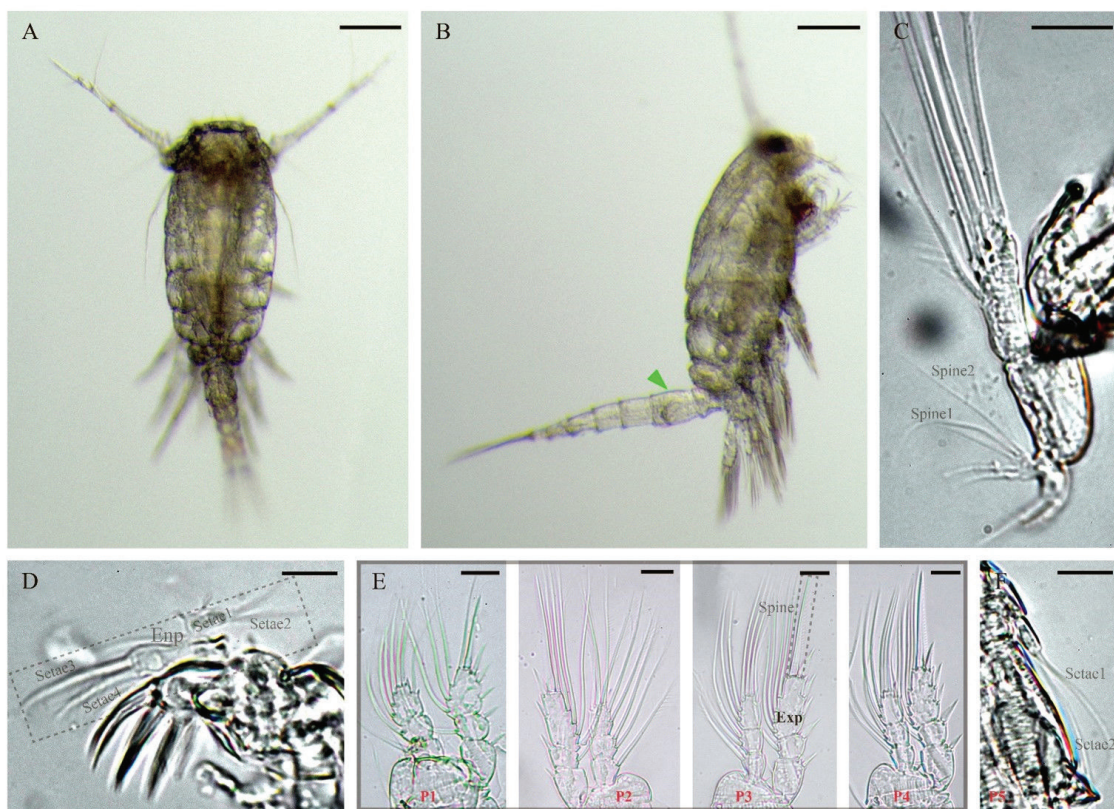


Fig. 4: Main morphological characteristics of *Dioithona oculata*, fixed male specimens. A) Dorsal view. B) Lateral view (green arrowhead depicts genital somite in the urosome). C) Mandible. D) Maxillule. E) P1 - P4 swimming legs. F) P5 leg. Enp - endopod; Exp - exopod. Scale bars for A, B - 100 μ m; for C, D, E, F - 20 μ m.

in female and male specimens and are in agreement with the original description (Farran, 1913), with the classification system of Razouls *et al.* (2005-2021), and the description made by Terbiyik Kurt (2018). The mandible (Md) has two spinulose spines in the basis (Figs. 3C, 4C); the endopod of the maxillule (Mx1) has four setae (Figs. 4C, 4D), the length of the terminal spine of the third segment of the swimming legs from 1 to 4 (P1-P4) is longer than the third exopod segment (Figs. 3E, 4E), the inner edge setae of the first exopod segment of P1-P4 is very small, and leg 5 (P5) has two setae (Figs. 3F, 4F).

Morphology of Oithona davisae

The TL of the female specimens was $550 \pm 3 \mu\text{m}$ ($n = 10$). The anterior part of the prosome is rounded in dor-

sal view and two small eye lenses are present; the lenses are blue in formalin-fixed specimens and black in living specimens (Fig. 5A). Females present a curved and sharply pointed rostrum that is visible in lateral view (Fig. 5B, C). The following female morphological characteristics agree with the original description (Ferrari & Orsi, 1984), and the descriptions by Temnykh & Nishida (2012), Cornils & Wend-Heckmann (2015) and Üstün & Terbiyik Kurt (2016). The Md has thick, curved, and blunt distal spines (Fig. 5D), the endopod of the Mx1 has one long seta, the swimming legs P1-P3 present the same number of spines on the outer margin of the exopod (1,1,3), while P4 presents formula 1,1,2 (Fig. 5E).

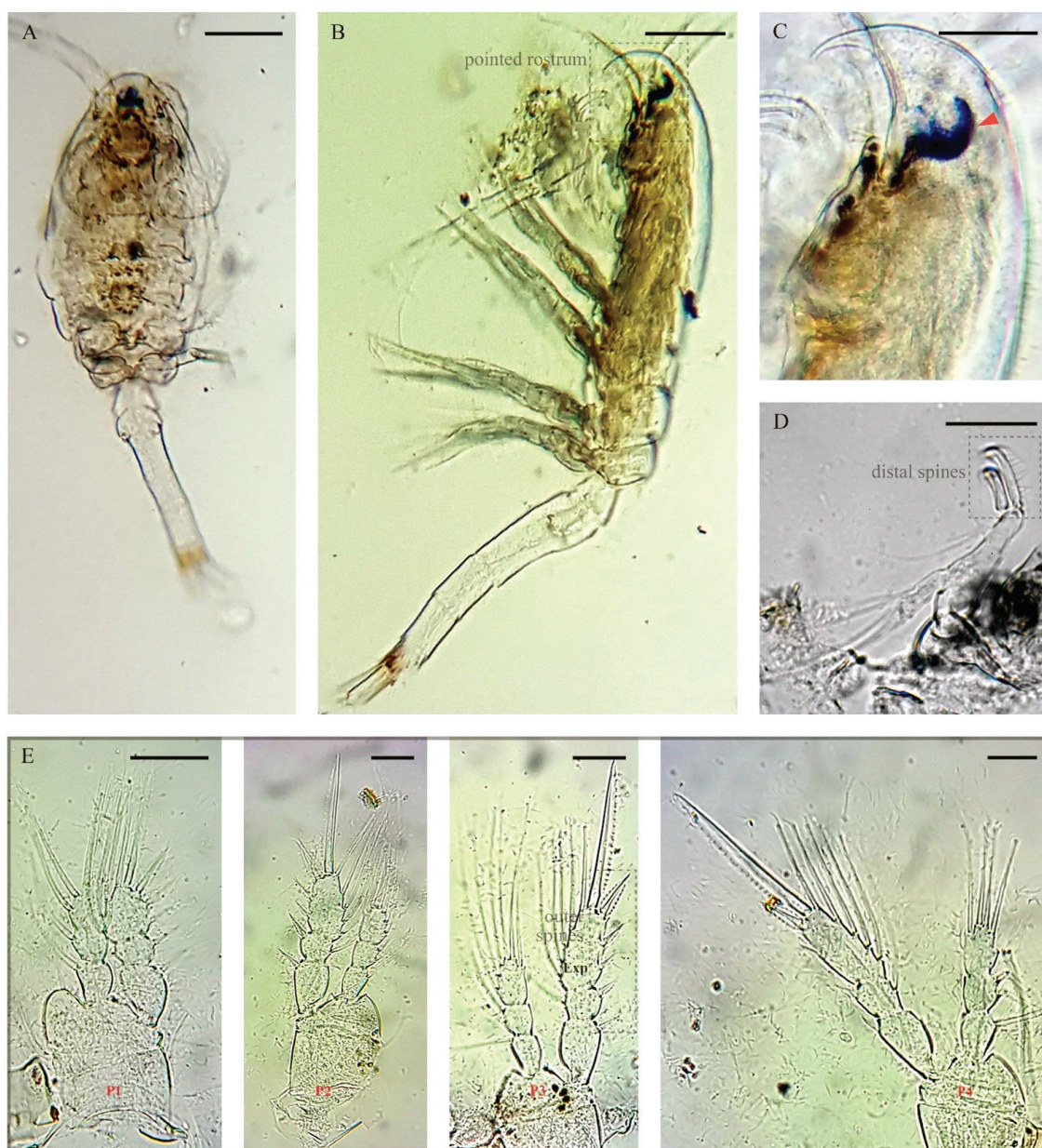


Fig. 5: Main morphological characteristics of *Oithona davisae*, fixed female specimens. A) Dorsal view. B) Lateral view. C) Enlarged view of curved and sharply pointed rostrum (red arrowhead depicts small blue eye lenses). D) Mandible. E) P1 - P4 swimming legs. Exp - exopod. Scale bars for A, B - $50 \mu\text{m}$; for C, D, E - $20 \mu\text{m}$.

Barcoding and phylogenetic inference

A total of 32 sequences of Oithonidae were analyzed (Table 3), including 12 sequences of *D. oculata*, of which four sequences were from Hawaii, five from Israel and three from Turkey (the last eight sequences obtained in this study). Additionally, 20 sequences of *O. davisae* were included, of which five sequences were from Israel (obtained in this study), three from Turkey (Aegean Sea, obtained in this study), ten from the North Sea and two from California. One sequence of *Paracyclops chiltoni* was used as an outgroup. The analysis using the Maximum Likelihood method produced a phylogenetic tree showing two *D. oculata* clades (Fig. 6). The first clade included the sequences obtained from Israel and Turkey, presenting congruence with a high bootstrap value of 99%. The second clade clustered the sequences from

Hawaiian specimens (Fig. 6). The sequences of *O. davisae* diverged from the sequences of *D. oculata*, forming a separate and single clade that included sequences from Israel, Turkey, North Sea and California, showing a high bootstrap value of 99% (Fig. 6).

The pairwise distance matrix (Table 4) confirmed the genetic similarity of the *D. oculata* specimens from Israel and Turkey and that of *O. davisae* specimens from Israel, Turkey, the North Sea and California, showing a low intraspecific distance value between 0-0.005 and 0-0.007, respectively. The sequences of *D. oculata* from Hawaii showed a higher genetic distance (0.260-0.269) from the sequences of *D. oculata* obtained in this study, indicating cryptic speciation within *D. oculata*. The selected outgroup displayed the maximum genetic distance, corroborating the intergeneric divergence (Table 4).

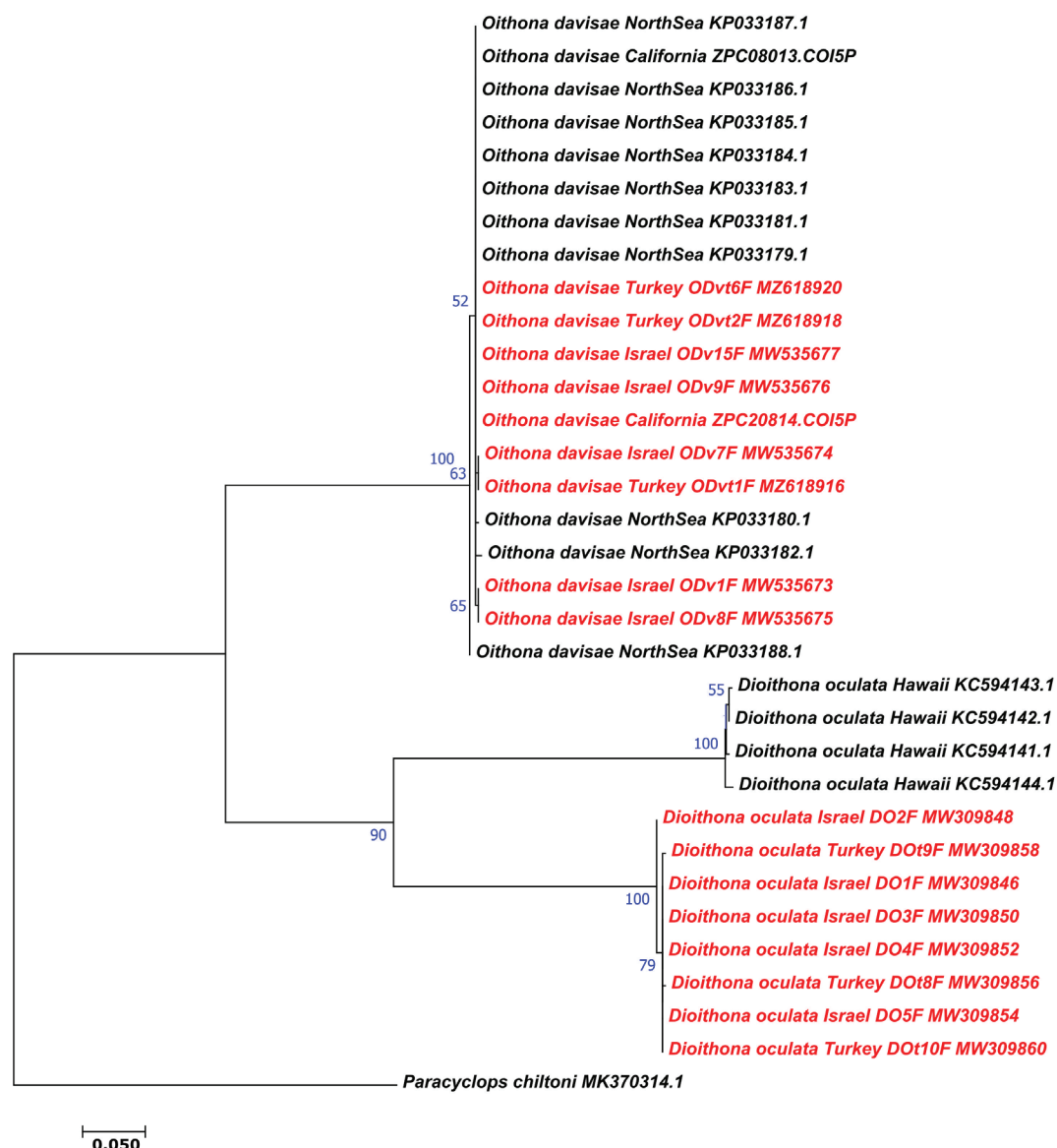


Fig. 6: Phylogenetic analysis and molecular identification of *Dioithona oculata* and *Oithona davisae* based on the mitochondrial COI gene. Phylogeny was inferred by Maximum Likelihood method based on the best-fitting model (HYK+I). The percentage of trees in which the associated taxa clustered together is shown next to the branches (bootstrapping=1000, only values above 50% are displayed).

Table 4. Pairwise genetic distance matrix of *COI* sequences between sequences of *Dioithona oculata*, *Oithona daviseae* and *Paracyclops chiltoni* (outgroup). P-distances and standard errors are respectively displayed in the below and above the diagonal, respectively.

| | 1 | 2 | 3 | 4 | 5 | 6 | 7 | 8 | 9 | 10 | 11 | 12 | 13 | 14 | 15 | 16 | 17 | 18 | 19 | 20 | 21 | 22 | 23 | 24 | 25 | 26 | 27 | 28 | 29 | 30 | 31 | 32 | 33 |
|----|--|---|-------|-------|-------|-------|-------|-------|-------|-------|-------|-------|-------|-------|-------|-------|-------|-------|-------|-------|-------|-------|-------|-------|-------|-------|-------|-------|-------|-------|-------|-------|-------|
| 1 | 0.005 | <i>D. oculata</i> Israel DO1F_MW309846 | 0.003 | 0.000 | 0.000 | 0.002 | 0.002 | 0.000 | 0.020 | 0.020 | 0.020 | 0.020 | 0.020 | 0.020 | 0.020 | 0.020 | 0.020 | 0.020 | 0.020 | 0.020 | 0.020 | 0.020 | 0.020 | 0.020 | 0.020 | 0.020 | 0.020 | 0.020 | 0.020 | 0.020 | 0.020 | 0.020 | 0.021 |
| 2 | | <i>D. oculata</i> Israel DO2F_MW309848 | 0.003 | 0.003 | 0.003 | 0.004 | 0.004 | 0.003 | 0.020 | 0.020 | 0.020 | 0.020 | 0.020 | 0.020 | 0.020 | 0.020 | 0.020 | 0.020 | 0.020 | 0.020 | 0.020 | 0.020 | 0.020 | 0.020 | 0.020 | 0.020 | 0.020 | 0.020 | 0.020 | 0.020 | 0.020 | 0.020 | 0.021 |
| 3 | | <i>D. oculata</i> Israel DO3F_MW309850 | 0.000 | 0.005 | 0.000 | 0.000 | 0.002 | 0.002 | 0.000 | 0.020 | 0.020 | 0.020 | 0.020 | 0.020 | 0.020 | 0.020 | 0.020 | 0.020 | 0.020 | 0.020 | 0.020 | 0.020 | 0.020 | 0.020 | 0.020 | 0.020 | 0.020 | 0.020 | 0.020 | 0.020 | 0.020 | 0.020 | 0.021 |
| 4 | | <i>D. oculata</i> Israel DO4F_MW309852 | 0.000 | 0.005 | 0.000 | 0.000 | 0.002 | 0.002 | 0.000 | 0.020 | 0.020 | 0.020 | 0.020 | 0.020 | 0.020 | 0.020 | 0.020 | 0.020 | 0.020 | 0.020 | 0.020 | 0.020 | 0.020 | 0.020 | 0.020 | 0.020 | 0.020 | 0.020 | 0.020 | 0.020 | 0.020 | 0.020 | 0.020 |
| 5 | <i>D. oculata</i> Israel DO5F_MW309854 | 0.000 | 0.005 | 0.000 | 0.000 | 0.002 | 0.002 | 0.000 | 0.020 | 0.020 | 0.020 | 0.020 | 0.020 | 0.020 | 0.020 | 0.020 | 0.020 | 0.020 | 0.020 | 0.020 | 0.020 | 0.020 | 0.020 | 0.020 | 0.020 | 0.020 | 0.020 | 0.020 | 0.020 | 0.020 | 0.020 | 0.020 | 0.021 |
| 6 | <i>D. oculata</i> Turkey DO6F_MW309856 | 0.002 | 0.007 | 0.002 | 0.002 | 0.005 | 0.003 | 0.002 | 0.020 | 0.020 | 0.020 | 0.020 | 0.020 | 0.020 | 0.020 | 0.020 | 0.020 | 0.020 | 0.020 | 0.020 | 0.020 | 0.020 | 0.020 | 0.020 | 0.020 | 0.020 | 0.020 | 0.020 | 0.020 | 0.020 | 0.020 | 0.020 | 0.021 |
| 7 | <i>D. oculata</i> Turkey DO9F_MW309858 | 0.002 | 0.007 | 0.002 | 0.002 | 0.005 | 0.002 | 0.020 | 0.020 | 0.020 | 0.020 | 0.020 | 0.020 | 0.020 | 0.020 | 0.020 | 0.020 | 0.020 | 0.020 | 0.020 | 0.020 | 0.020 | 0.020 | 0.020 | 0.020 | 0.020 | 0.020 | 0.020 | 0.020 | 0.020 | 0.020 | 0.020 | 0.021 |
| 8 | <i>D. oculata</i> Turkey DO10F_MW309860 | 0.000 | 0.005 | 0.000 | 0.000 | 0.000 | 0.002 | 0.002 | 0.020 | 0.020 | 0.020 | 0.020 | 0.020 | 0.020 | 0.020 | 0.020 | 0.020 | 0.020 | 0.020 | 0.020 | 0.020 | 0.020 | 0.020 | 0.020 | 0.020 | 0.020 | 0.020 | 0.020 | 0.020 | 0.020 | 0.020 | 0.020 | 0.021 |
| 9 | <i>D. oculata</i> Hawaii KC594141.1 | 0.267 | 0.267 | 0.267 | 0.267 | 0.267 | 0.267 | 0.267 | 0.267 | 0.004 | 0.004 | 0.003 | 0.022 | 0.022 | 0.022 | 0.022 | 0.022 | 0.022 | 0.022 | 0.022 | 0.022 | 0.022 | 0.022 | 0.022 | 0.022 | 0.022 | 0.022 | 0.022 | 0.022 | 0.022 | 0.022 | 0.022 | 0.022 |
| 10 | <i>D. oculata</i> Hawaii KC594144.1 | 0.262 | 0.264 | 0.262 | 0.262 | 0.264 | 0.262 | 0.262 | 0.262 | 0.009 | 0.005 | 0.005 | 0.022 | 0.022 | 0.022 | 0.022 | 0.022 | 0.022 | 0.022 | 0.022 | 0.022 | 0.022 | 0.022 | 0.022 | 0.022 | 0.022 | 0.022 | 0.022 | 0.022 | 0.022 | 0.022 | 0.022 | 0.022 |
| 11 | <i>D. oculata</i> Hawaii KC594143.1 | 0.260 | 0.260 | 0.260 | 0.260 | 0.262 | 0.260 | 0.260 | 0.260 | 0.007 | 0.011 | 0.002 | 0.022 | 0.022 | 0.022 | 0.022 | 0.022 | 0.022 | 0.022 | 0.022 | 0.022 | 0.022 | 0.022 | 0.022 | 0.022 | 0.022 | 0.022 | 0.022 | 0.022 | 0.022 | 0.022 | 0.022 | 0.022 |
| 12 | <i>D. oculata</i> Hawaii KC594142.1 | 0.262 | 0.262 | 0.262 | 0.262 | 0.264 | 0.262 | 0.262 | 0.262 | 0.005 | 0.009 | 0.002 | 0.022 | 0.022 | 0.022 | 0.022 | 0.022 | 0.022 | 0.022 | 0.022 | 0.022 | 0.022 | 0.022 | 0.022 | 0.022 | 0.022 | 0.022 | 0.022 | 0.022 | 0.022 | 0.022 | 0.022 | 0.022 |
| 13 | <i>O. danivae</i> Israel ODv1F_MW535673 | 0.289 | 0.285 | 0.289 | 0.289 | 0.289 | 0.292 | 0.289 | 0.289 | 0.303 | 0.303 | 0.303 | 0.003 | 0.000 | 0.002 | 0.002 | 0.003 | 0.002 | 0.002 | 0.002 | 0.002 | 0.002 | 0.003 | 0.002 | 0.002 | 0.002 | 0.002 | 0.002 | 0.002 | 0.002 | 0.004 | 0.002 | 0.002 |
| 14 | <i>O. danivae</i> Israel ODv7F_MW535674 | 0.294 | 0.289 | 0.294 | 0.294 | 0.294 | 0.296 | 0.294 | 0.294 | 0.308 | 0.310 | 0.308 | 0.308 | 0.005 | 0.003 | 0.002 | 0.002 | 0.000 | 0.002 | 0.002 | 0.002 | 0.002 | 0.002 | 0.002 | 0.004 | 0.002 | 0.002 | 0.002 | 0.002 | 0.002 | 0.004 | 0.002 | 0.002 |
| 15 | <i>O. danivae</i> Israel ODv8F_MW535675 | 0.289 | 0.285 | 0.289 | 0.289 | 0.289 | 0.292 | 0.289 | 0.289 | 0.303 | 0.303 | 0.303 | 0.000 | 0.005 | 0.002 | 0.002 | 0.003 | 0.002 | 0.002 | 0.002 | 0.002 | 0.002 | 0.002 | 0.002 | 0.004 | 0.002 | 0.002 | 0.002 | 0.002 | 0.002 | 0.004 | 0.002 | 0.002 |
| 16 | <i>O. danivae</i> Israel ODv9F_MW535676 | 0.292 | 0.287 | 0.292 | 0.292 | 0.292 | 0.294 | 0.292 | 0.292 | 0.305 | 0.308 | 0.305 | 0.002 | 0.002 | 0.002 | 0.002 | 0.000 | 0.002 | 0.002 | 0.002 | 0.002 | 0.002 | 0.002 | 0.003 | 0.000 | 0.000 | 0.000 | 0.000 | 0.000 | 0.000 | 0.000 | 0.000 | 0.002 |
| 17 | <i>O. danivae</i> Israel ODv15F_MW535677 | 0.292 | 0.287 | 0.292 | 0.292 | 0.292 | 0.294 | 0.292 | 0.292 | 0.305 | 0.308 | 0.305 | 0.002 | 0.002 | 0.002 | 0.000 | 0.002 | 0.002 | 0.002 | 0.002 | 0.002 | 0.002 | 0.002 | 0.004 | 0.002 | 0.002 | 0.002 | 0.002 | 0.002 | 0.002 | 0.004 | 0.002 | 0.002 |
| 18 | <i>O. danivae</i> Turkey ODv1F_MZ618916 | 0.294 | 0.289 | 0.294 | 0.294 | 0.294 | 0.296 | 0.294 | 0.294 | 0.308 | 0.310 | 0.308 | 0.308 | 0.005 | 0.000 | 0.005 | 0.002 | 0.002 | 0.002 | 0.002 | 0.002 | 0.002 | 0.002 | 0.004 | 0.002 | 0.002 | 0.002 | 0.002 | 0.002 | 0.004 | 0.002 | 0.002 | 0.002 |
| 19 | <i>O. danivae</i> Turkey ODv2F_MZ618918 | 0.292 | 0.287 | 0.292 | 0.292 | 0.292 | 0.294 | 0.292 | 0.292 | 0.305 | 0.308 | 0.305 | 0.002 | 0.002 | 0.002 | 0.000 | 0.000 | 0.002 | 0.002 | 0.000 | 0.000 | 0.000 | 0.003 | 0.000 | 0.000 | 0.000 | 0.000 | 0.000 | 0.000 | 0.000 | 0.000 | 0.000 | 0.002 |
| 20 | <i>O. danivae</i> Turkey ODv6F_MZ618920 | 0.292 | 0.287 | 0.292 | 0.292 | 0.292 | 0.294 | 0.292 | 0.292 | 0.305 | 0.308 | 0.305 | 0.002 | 0.002 | 0.002 | 0.000 | 0.000 | 0.002 | 0.002 | 0.000 | 0.000 | 0.000 | 0.003 | 0.000 | 0.000 | 0.000 | 0.000 | 0.000 | 0.000 | 0.000 | 0.000 | 0.000 | 0.002 |
| 21 | <i>O. danivae</i> NorthSea KP033179.1 | 0.292 | 0.287 | 0.292 | 0.292 | 0.292 | 0.294 | 0.292 | 0.292 | 0.305 | 0.308 | 0.305 | 0.002 | 0.002 | 0.002 | 0.000 | 0.000 | 0.002 | 0.002 | 0.000 | 0.000 | 0.000 | 0.003 | 0.000 | 0.000 | 0.000 | 0.000 | 0.000 | 0.000 | 0.003 | 0.000 | 0.000 | 0.002 |
| 22 | <i>O. danivae</i> NorthSea KP033180.1 | 0.294 | 0.289 | 0.294 | 0.294 | 0.294 | 0.296 | 0.294 | 0.294 | 0.308 | 0.310 | 0.308 | 0.308 | 0.005 | 0.005 | 0.002 | 0.000 | 0.002 | 0.005 | 0.002 | 0.002 | 0.002 | 0.004 | 0.002 | 0.000 | 0.000 | 0.000 | 0.000 | 0.000 | 0.003 | 0.000 | 0.000 | 0.002 |
| 23 | <i>O. danivae</i> NorthSea KP033181.1 | 0.292 | 0.287 | 0.292 | 0.292 | 0.292 | 0.294 | 0.292 | 0.292 | 0.305 | 0.308 | 0.305 | 0.002 | 0.002 | 0.002 | 0.000 | 0.000 | 0.002 | 0.002 | 0.005 | 0.002 | 0.002 | 0.004 | 0.002 | 0.002 | 0.002 | 0.002 | 0.002 | 0.002 | 0.004 | 0.002 | 0.002 | 0.002 |
| 24 | <i>O. danivae</i> NorthSea KP033182.1 | 0.294 | 0.289 | 0.294 | 0.294 | 0.294 | 0.296 | 0.294 | 0.294 | 0.308 | 0.310 | 0.308 | 0.308 | 0.007 | 0.007 | 0.005 | 0.005 | 0.007 | 0.005 | 0.005 | 0.005 | 0.007 | 0.003 | 0.000 | 0.000 | 0.000 | 0.000 | 0.000 | 0.000 | 0.003 | 0.004 | 0.003 | 0.003 |
| 25 | <i>O. danivae</i> NorthSea KP033183.1 | 0.292 | 0.287 | 0.292 | 0.292 | 0.292 | 0.294 | 0.292 | 0.292 | 0.305 | 0.308 | 0.305 | 0.002 | 0.002 | 0.002 | 0.000 | 0.000 | 0.002 | 0.002 | 0.005 | 0.002 | 0.002 | 0.003 | 0.000 | 0.000 | 0.000 | 0.000 | 0.000 | 0.000 | 0.003 | 0.000 | 0.000 | 0.002 |
| 26 | <i>O. danivae</i> NorthSea KP033184.1 | 0.292 | 0.287 | 0.292 | 0.292 | 0.292 | 0.294 | 0.292 | 0.292 | 0.305 | 0.308 | 0.305 | 0.002 | 0.002 | 0.002 | 0.000 | 0.000 | 0.002 | 0.002 | 0.005 | 0.002 | 0.002 | 0.005 | 0.000 | 0.000 | 0.000 | 0.000 | 0.000 | 0.000 | 0.003 | 0.000 | 0.000 | 0.002 |
| 27 | <i>O. danivae</i> NorthSea KP033185.1 | 0.292 | 0.287 | 0.292 | 0.292 | 0.292 | 0.294 | 0.292 | 0.292 | 0.305 | 0.308 | 0.305 | 0.002 | 0.002 | 0.002 | 0.000 | 0.000 | 0.002 | 0.002 | 0.005 | 0.002 | 0.002 | 0.005 | 0.000 | 0.000 | 0.000 | 0.000 | 0.000 | 0.000 | 0.003 | 0.000 | 0.000 | 0.002 |
| 28 | <i>O. danivae</i> NorthSea KP033186.1 | 0.292 | 0.287 | 0.292 | 0.292 | 0.292 | 0.294 | 0.292 | 0.292 | 0.305 | 0.308 | 0.305 | 0.002 | 0.002 | 0.002 | 0.000 | 0.000 | 0.002 | 0.002 | 0.005 | 0.002 | 0.002 | 0.005 | 0.000 | 0.000 | 0.000 | 0.000 | 0.000 | 0.000 | 0.003 | 0.000 | 0.000 | 0.002 |
| 29 | <i>O. danivae</i> NorthSea KP033187.1 | 0.292 | 0.287 | 0.292 | 0.292 | 0.292 | 0.294 | 0.292 | 0.292 | 0.305 | 0.308 | 0.305 | 0.002 | 0.002 | 0.002 | 0.000 | 0.000 | 0.002 | 0.002 | 0.005 | 0.002 | 0.002 | 0.005 | 0.000 | 0.000 | 0.000 | 0.000 | 0.000 | 0.000 | 0.003 | 0.000 | 0.000 | 0.002 |
| 30 | <i>O. danivae</i> NorthSea KP033188.1 | 0.292 | 0.287 | 0.292 | 0.292 | 0.292 | 0.294 | 0.292 | 0.292 | 0.305 | 0.308 | 0.305 | 0.007 | 0.007 | 0.005 | 0.005 | 0.007 | 0.005 | 0.005 | 0.005 | 0.005 | 0.007 | 0.005 | 0.009 | 0.005 | 0.005 | 0.005 | 0.005 | 0.005 | 0.005 | 0.003 | 0.003 | 0.003 |
| 31 | <i>O. danivae</i> California ZFC08013.C015P | 0.292 | 0.287 | 0.292 | 0.292 | 0.292 | 0.294 | 0.292 | 0.292 | 0.305 | 0.308 | 0.305 | 0.002 | 0.002 | 0.002 | 0.000 | 0.000 | 0.002 | 0.002 | 0.005 | 0.002 | 0.002 | 0.000 | 0.000 | 0.000 | 0.000 | 0.000 | 0.000 | 0.000 | 0.000 | 0.000 | 0.000 | 0.002 |
| 32 | <i>O. danivae</i> California ZFC20814.C015P | 0.292 | 0.287 | 0.292 | 0.292 | 0.292 | 0.294 | 0.292 | 0.292 | 0.305 | 0.308 | 0.305 | 0.002 | 0.002 | 0.002 | 0.000 | 0.000 | 0.002 | 0.002 | 0.005 | 0.002 | 0.002 | 0.000 | 0.000 | 0.000 | 0.000 | 0.000 | 0.000 | 0.000 | 0.000 | 0.000 | 0.000 | 0.002 |
| 33 | <i>Paracystis chiliani</i> MK37031.1 | 0.335 | 0.337 | 0.335 | 0.335 | 0.335 | 0.337 | 0.335 | 0.335 | 0.349 | 0.351 | 0.344 | 0.333 | 0.333 | 0.333 | 0.330 | 0.333 | 0.330 | 0.333 | 0.330 | 0.330 | 0.328 | 0.330 | 0.333 | 0.330 | 0.330 | 0.330 | 0.330 | 0.330 | 0.328 | 0.330 | 0.330 | 0.330 |

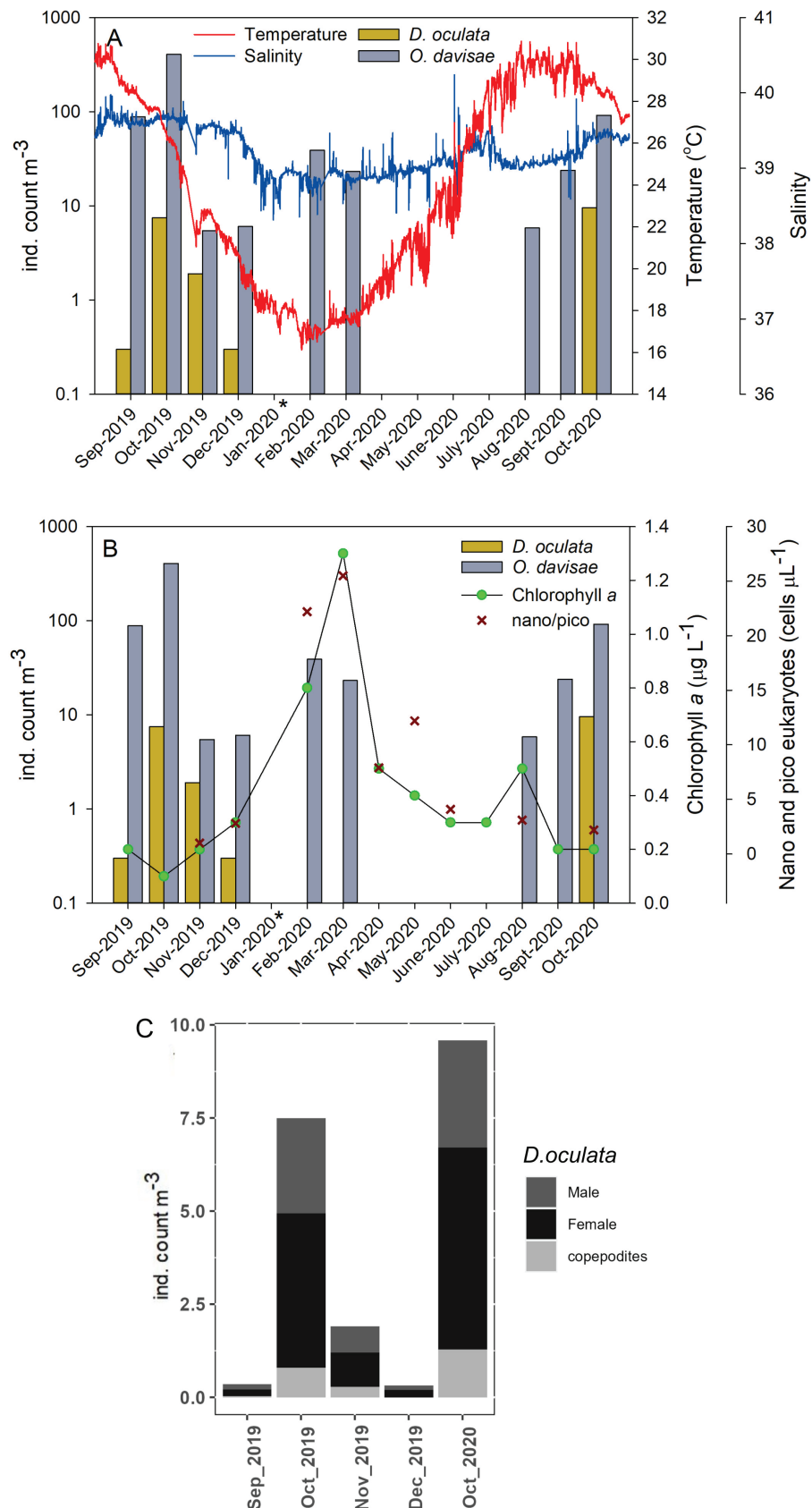


Fig. 7: Temporal variation of *Dioithona oculata* and *Oithona davisae* at the Hadera station, during September 2019-October 2020. A-B) Seasonal dynamics of *D. oculata* and *O. davisae*. In A, the red line shows seawater temperature and the blue line - salinity, In B, the x symbols represent monthly averages of chlorophyll *a* (converted from fluorescence). Circles represent the pico and nano-eukaryote abundances in each month sampled. * denotes no sampling. Temperature, salinity, and fluorescence measurements were continuously recorded (in 10 min intervals) by a fixed CTD at 13 m depth. C) Seasonal variation of male, female, and copepodite abundances.

Species abundances and temporal variation

Dioithona oculata exhibited a marked seasonal pattern at the Hadera site, appearing only from September to December 2019 and in October 2020 (Fig. 7A). This species was more abundant in October 2019 and 2020, with abundances of 7 and 10 ind. m⁻³, respectively. Throughout the time *D. oculata* was observed in Hadera site, females outnumbered males (Fig. 7C), showing an average sex ratio of 1.50 ± 0.27 (females:males). *D. oculata* copepodites were also observed in Hadera (the stage was not distinguished) and were highly abundant in October (Fig. 7C). In the shallow waters of the Qishon Harbour, *D. oculata* was observed in October 2020, displaying an abundance of 695 ind. m⁻³, 3-4 orders of magnitude higher than in Hadera site. *O. davisae* was observed almost all year, from September 2019 to October 2020 at the Hadera site (Fig. 7A), showing the highest abundances in October 2019 and October 2020 (406 and 92 ind. m⁻³, respectively). This species was also recorded in October 2020 at Qishon Harbour, exhibiting an abundance of 6×10^4 ind. m⁻³.

Interaction with environmental parameters

At the Hadera site, *D. oculata* exhibited the highest abundance in October 2019 and 2020 when the water temperature reached 28.0 ± 0.6 °C, and the lowest abundance in December 2019, at 21.0 ± 1.1 °C (Fig. 7A). *O. davisae* peaked in October 2019 and 2020. However, no significant positive correlation was found between *D. oculata* and *O. davisae* abundance and temperature ($p > 0.05$, Table 5). The salinity at the Hadera site varied little throughout the year (38-40.5, Fig. 7A). However, there was a significant positive correlation between salinity and the abundance of *D. oculata* ($p < 0.05$, Table 5). The abundance of *D. oculata* was significantly and negatively correlated with chlorophyll *a* and pico- and nano-eukaryotes (Fig. 7B, Table 5), whereas *O. davisae* did not show any association with these variables.

Table 5. Abundances of *Dioithona oculata* and *Oithona davisae*, and environmental parameters measured in Hadera, during September 2019 – October 2020. Temperature, salinity and fluorescence (converted to $\mu\text{g L}^{-1}$ Chlorophyll *a*) were continuously recorded with a fixed CTD at 13 m depth. Monthly means and standard deviations are presented. Correlations between the oithonid abundances and the environmental parameters are presented by Spearman Correlation Coefficient *R* and corresponding *p*-value.

| Month | Abundance ind. m ⁻³ | Temperature (°C) | Salinity | Chloro- phyll <i>a</i> $\mu\text{g L}^{-1}$ | Pico- & nano-eu- karyotes | | | | |
|----------------------|-----------------------------------|------------------------------------|--|---|--|-----|------|-----|----------------------|
| | <i>D. oculata</i> | <i>O. davisae</i> | Mean | SD | Mean | SD | Mean | SD | cells/ μl |
| September_2019 | 0.4 | 89 | 29.5 | 0.7 | 39.6 | 0.1 | 0.2 | 0.3 | NA |
| October_2019 | 7 | 406 | 27.5 | 0.7 | 39.6 | 0.0 | 0.1 | 0.1 | NA |
| November_2019 | 2 | 5 | 23.9 | 1.5 | 39.6 | 0.1 | 0.2 | 0.1 | 1.0 |
| December_2019 | 0.3 | 6 | 20.7 | 1.1 | 39.4 | 0.1 | 0.3 | 0.1 | 2.8 |
| February_2020 | 0.00 | 31 | 17.3 | 0.5 | 38.9 | 0.1 | 0.8 | 0.6 | 22.2 |
| March_2020 | 0.00 | 23 | 17.6 | 0.2 | 38.9 | 0.1 | 1.3 | 0.5 | 25.5 |
| April_2020 | 0.00 | 0.0 | 19.3 | 0.8 | 38.9 | 0.1 | 0.5 | 0.3 | 7.9 |
| May_2020 | 0.00 | 0.0 | 21.3 | 1.0 | 39.0 | 0.1 | 0.4 | 0.2 | 12.2 |
| June_2020 | 0.00 | 0.0 | 24.5 | 1.6 | 39.2 | 0.1 | 0.3 | 0.1 | 4.1 |
| July_2020 | 0.00 | 0.0 | 28.3 | 0.8 | 39.2 | 0.2 | 0.3 | 0.1 | NA |
| August_2020 | 0.00 | 6 | 29.8 | 0.4 | 39.1 | 0.0 | 0.5 | 0.5 | 3.1 |
| September_2020 | 0.00 | 24 | 29.4 | 0.5 | 39.2 | 0.0 | 0.2 | 0.1 | NA |
| October_2020 | 10 | 92 | 28.0 | 0.6 | 39.4 | 0.0 | 0.2 | 0.1 | 2.2 |
| Spearman correlation | <i>D. oculata</i> | <i>R</i> = 0.2 <i>p</i> = 0.51 | <i>R</i> = 0.82 <i>p</i> = 0.0006 | <i>R</i> = - 0.78 <i>p</i> = 0.0021 | <i>R</i> = -0.82 <i>p</i> = 0.007 | | | | |
| | <i>O. davisae</i> | <i>R</i> = 0.17 <i>p</i> = 0.58 | <i>R</i> = 0.44 <i>p</i> = 0.13 | <i>R</i> = -0.38 <i>p</i> = 0.20 | <i>R</i> = -0.034 <i>p</i> = 0.83 | | | | |

Discussion

Taxonomy and phylogenetic interference

D. oculata and *O. davisae* are reported here for the first time as non-native cyclopoid copepods inhabiting Israeli coastal waters. Our morphological identification is supported by DNA barcoding. However, the *COI*-based phylogeny suggests that *D. oculata* might be a species complex containing at least two lineages, one formed by the species found in the EMS and another from the Western Pacific Ocean. We compared the sequences obtained in this study with the only previously existing sequences of *D. oculata* provided by Jungbluth & Lenz (2013). These authors did not provide a morphological description of the specimens found in Kaneohe Bay (Hawaii), but indicated that the specimens of *D. oculata* were identified following the description made by Nishida (1985).

We did not find differences in the morphological characteristics of the specimens found in Israel and Turkey (Terbiyik Kurt, 2018) and the specimens described by Nishida (1985). *D. oculata* was originally described by Farran (1913) as *Oithona oculata*, but Kiefer (1935) observed that specimens of this species presented two setae on the free segment of leg 5 (P5) instead of one, as in *Oithona*, and created the genus *Dioithona*. The creation of this genus, based on morphological characters, has been disputed because a delineation based on a single character is too restrictive (Vervoort, 1964; Wellershaus, 1969; Nishida, 1985; Boxshall & Halsey, 2004), suggesting that the genus *Dioithona* should be revised. We performed species delimitation analyses with *Oithona* and *Dioithona* species (not included in this study, *in prep*) and combined these analyses with a review of the taxonomic features to validate the genus *Dioithona*. Moreover, molecular studies have shown that many widespread species represent a group of several cryptic or pseudocryptic species, instead of a single species (Andrews *et al.*, 2014). There is clear evidence that some pelagic copepods form cryptic species (Cornils & Held, 2014; Cornils *et al.*, 2017) because of the presence of barriers (e.g., landmasses, oceanic gyres, environmental variables) to gene flow in the oceans (Chen & Hare, 2011; Stupnikova *et al.*, 2013). *D. oculata* is distributed worldwide and may have speciated in different oceanic regions.

In the case of *O. davisae*, we did not find morphological differences between the specimens found in this study and those originally described by Ferrari & Orsi (1984), as well as the specimens introduced in other areas of the Mediterranean Sea (Temnykh & Nishida, 2012; Üstün & Terbiyik Kurt, 2016) and the Atlantic Ocean (Cornils & Wend-Heckmann, 2015). The morphological taxonomy was highly supported by the phylogenetic analysis, which clearly showed an identical genetic composition of the populations from the North Sea, Northeast Pacific Ocean (California), Aegean Sea (Turkey) and Levantine Sea.

In the Israeli Mediterranean Sea, oithonid copepods have been found in high densities in coastal waters (Kimor & Wood, 1975) and open sea (Mazzocchi *et al.*, 2014). However, previous records of oithonid species in

the Levantine Sea reported *O. plumifera*, *O. setigera*, *O. atlantica*, *O. longispina*, *O. similis*, and *O. tenuis*, and none of the species found in the present study. *D. oculata* represents the first diothonid species described from Israeli coastal waters. This species was first found in 2018 in the northeastern Mediterranean Sea coastal waters (Terbiyik Kurt, 2018). In contrast, *O. davisae* was first recorded in 2001 in the Black Sea. Initially, this species was described as *Oithona brevicornis* (Zagorodnyaya, 2002), but later, in 2012, Temnykh & Nishida identified it as *O. davisae*. Subsequently, this species has been reported in the coastal waters of the central Mediterranean Sea (Zagami *et al.*, 2018), Adriatic Sea (Vidjak *et al.*, 2019) and Aegean Sea (Dragicevic *et al.*, 2019; Terbiyik Kurt & Beşiktepe, 2019). However, the present record of *O. davisae* extends its distribution area to the easternmost Mediterranean Sea.

Species introductions in the Mediterranean Sea

D. oculata was first recorded in the Mediterranean Sea in Turkish coastal waters by Terbiyik Kurt (2018), who suggested that it was introduced to the northeast Levantine Sea by ballast waters due to the increase in maritime trade in Iskenderun Bay (Çinar *et al.*, 2005), rather than by direct introduction via the Suez Canal, as the species was absent from the southern part of the basin. However, in the present study, the first study since the 1970s that reports on copepod species in Israeli coastal waters, we found this species in two sites with different environmental characteristics. Our findings indicate that *D. oculata* has likely been introduced to the Levantine Sea via the Suez Canal and has spread across the EMS by the long-shore current, which circulates anticlockwise (Robinson *et al.*, 1992), allowing the propagation of pelagic species from the south to the northeast part of the Mediterranean Sea (Lasram *et al.*, 2008; Occhipinti-Ambrogia & Galil, 2010).

In contrast to *D. oculata*, *O. davisae* was likely introduced to the Mediterranean Sea via shipping, as indicated by other Mediterranean studies (Yıldız *et al.*, 2017; Zagami *et al.*, 2018; Terbiyik Kurt & Beşiktepe, 2019) and in other oceans (Cornils *et al.*, 2015). Ferrari & Orsi (1984) first recorded this species in San Francisco Bay, indicating that *O. davisae* arrived in the estuary by ship-ballast water transport from Asian harbours. This introduction vector was corroborated by Choi *et al.* (2005) who observed this species in ballast water tanks that were discharged in San Francisco Bay from ships originating in Japan. Cornils & Wend-Heckmann (2015) recorded the introduction of *O. davisae* into the North Sea via ballast waters, and Uriarte *et al.* (2016) confirmed the spread and establishment of this species in the Northeast Atlantic. These previous records and our study indicate that *O. davisae* was initially introduced to the Mediterranean Sea from the Northeast Atlantic, propagating its populations from west to east.

In its native range, *D. oculata* is a prominent and highly abundant component of mangrove swamps, reef habi-

tats, estuaries and coastal lagoons, which aggregates and forms dense swarms (Hammer & Carleton, 1979; Ambler, 2002; Hsu *et al.*, 2008). It can also inhabit offshore waters, albeit at lower densities than inshore habitats (Rezai *et al.*, 2004). Similarly, *O. davisae* is prominent in very shallow environments such as lagoons, coastal lakes, estuaries, inlets and bays where it can form dense aggregations (Hirota & Tanaka, 1985; Hirota, 1990; Uye & Sano, 1995, 1998). However, it can also be found in high densities in deeper coastal waters at a depth of ~20 m (Checkley *et al.*, 1992). In our study, *D. oculata* and *O. davisae* were found in coastal waters and most abundant in a harbour. Terbiyik Kurt (2018) recorded an abundance gradient of *D. oculata* along Iskenderun Bay, showing that this species is more abundant in very shallow environments than in deeper coastal waters, as was also found in this study. Terbiyik Kurt & Beşiktepe (2019) observed the same trend for *O. davisae* across the Turkish Aegean Sea.

Temporal variability of *D. oculata* and *O. davisae* in the southeastern Levantine Sea

We found *D. oculata* at the Israeli coast in the Levantine Sea between September and December 2019 and October 2020, and it was absent in the remaining months. In Iskenderun Bay (Turkish coastal waters), *D. oculata* was observed only in October, from 2013 to 2016 (Terbiyik Kurt, 2018); subsequently, this species was also observed in July 2018, and April and December 2019 (Terbiyik Kurt, 2020a). This variability may suggest that the occurrence of *D. oculata* in its invaded range may be temporally restricted by a narrow environmental factor range, being highly abundant in the warm-temperate period and exhibiting low abundances and/or absence in the cold season. In other coastal regions, such as the Straits of Malacca in Malaysia, *D. oculata* showed a similar pattern, with higher abundances from November to April, when the water column temperature ranged between 26 and 29 °C (Rezai *et al.*, 2004). However, *D. oculata* can survive at temperatures as low as 17 °C in its native and invaded distribution range, although at very low abundances (Lo *et al.*, 2004; Terbiyik Kurt, 2020a). In this study, *D. oculata* showed decreased abundances at the start of the winter (December 2019), when the temperature dropped to 21 °C, indicating a preference for warmer waters. Although we did not find a significant correlation with temperature, we infer that *D. oculata* prefers warm-temperate conditions to reproduce and maintain large population abundances in its native and colonized areas. Thus, the ongoing and predicted Mediterranean Sea warming may further facilitate the spread of this species westward. Physiological experiments should be conducted to further corroborate *D. oculata* thermal preferences.

O. davisae can survive and thrive in a wide range of thermal conditions (from 9 to 28 °C) in its native range of occurrence (Checkley *et al.*, 1992; Uye & Sano, 1995; 1998). Uye & Sano (1995; 1998) observed that in Japanese coastal waters, this species showed the highest abundance in summer when the water column temperature reached

28 °C, but it was also abundant in autumn, at 20 °C. In our study, *O. davisae* exhibited a similar pattern, with a peak in abundance at 28 °C, during October 2019 and October 2020, and in February 2020 at 17 °C. Terbiyik Kurt & Beşiktepe (2019) also observed that *O. davisae* in Izmir Bay (Turkish Aegean Sea) displayed high densities during the warmer period (27 °C, July and September), as well as when the water temperature decreased to 11.4 °C. The densities recorded by Terbiyik Kurt & Beşiktepe (2019) were lower than those in our study, likely due to the larger mesh size of the zooplankton net they used (200 µm vs. 65 µm in our study), thereby underestimating the abundance of small-sized oithonids. However, the temporal variation patterns were similar in both studies. These observations confirm the high thermal adaptability of *O. davisae* in the Mediterranean Sea, as demonstrated in several experimental and field studies in the Black Sea (Svetlichny *et al.*, 2016; Yıldız *et al.*, 2017; Svetlichny *et al.*, 2018), indicating that *O. davisae* maintains its eurythermal affinity even in its colonized areas.

Although salinity in the Israeli coastal waters has a narrow variability range (between 38 and 40.5), we observed a significant positive correlation between *D. oculata* abundance and salinity. Terbiyik Kurt (2018) also recorded the highest abundance of *D. oculata* under high salinity conditions (39.4), suggesting that salinity might play a role together with temperature in the temporal variability of *D. oculata* in the EMS. However, physiological experiments at different salinity levels should be performed to test whether salinity is a driving factor for the temporal variability of *D. oculata* populations. Our study did not find an association between salinity and *O. davisae* abundance. However, physiological experiments have shown that *O. davisae* is highly adapted to tolerate a wide salinity range (3–40) (Svetlichny & Hubareva, 2014; Zagami *et al.*, 2018; Svetlichny *et al.*, 2020).

The two non-native species recorded in this study showed increased densities in October 2019 and 2020, suggesting that they might not compete for space or resources (e.g., food) in Israeli coastal waters. This assumption can be explained by the fact that the two species occupy different trophic niches. *O. davisae* is smaller in size than *D. oculata* and is an ambush feeder that prefers to prey on heterotrophic flagellates and dinoflagellates (Henriksen *et al.*, 2007; Kiørboe, 2011). There are few detailed studies on the feeding behaviour and preferences of *D. oculata*. Santhosh *et al.* (2018) observed that in laboratory conditions, *D. oculata* feeds on microalgae but can also consume ciliates and similar protozoans. Buskey *et al.* (2004) observed that *D. oculata* prefers feeding on large cells, showing higher clearance rates when fed on ciliates and autotrophic dinoflagellates compared to heterotrophic dinoflagellates. In our study, *D. oculata* presented the highest abundance in October, when low chlorophyll *a* and pico- and nano-eukaryote values were recorded. These results suggest that *D. oculata* might feed on other food sources, such as larger protozooplankton, to maintain its large population, as was observed by Buskey *et al.* (2004) when phytoplankton availability is limited.

O. davisae did not show significant correlations with chlorophyll *a* and pico- and nano-eukaryotes. However, it has been observed that this species does not take up phytoplankton cells in proportion to its abundance in natural or artificial assemblages (Khanaychenko *et al.*, 2018), indicating that *O. davisae* does not feed on the most abundant cells. This species actively selects for motile cells such as heterotrophic dinoflagellates (Zamora-Terol & Saiz, 2013; Khanaychenko *et al.*, 2018). Additionally, *O. davisae* performs well at low food availability (Zamora-Terol & Saiz, 2013), and exhibits a low satiating threshold (Almeda *et al.*, 2010), which might explain the population peak during a period of food scarcity.

It has been previously shown that in winter, males are absent from the populations of *O. davisae*, and copepodites and females are less abundant (Svetlichny *et al.*, 2018; Svetlichny *et al.*, 2021). To overcome adverse conditions, *O. davisae* females can maintain viable sperm in the spermatheca for a long period (~2 months after mating) and lay fertilised eggs after the increase in water temperature (Hubareva & Svetlichny, 2013; Svetlichny *et al.*, 2016; Svetlichny *et al.*, 2018). This reproductive strategy might be the result of a reduction in male encounters when the population decreases (Kjørboe, 2007). *O. davisae* can reduce metabolic energy and locomotor activity (Svetlichny *et al.*, 2016, 2021), which might facilitate their survival under adverse conditions. These adaptations might be present in other related species from the same family, explaining how *D. oculata* could maintain their population in the period of the year when we detected negligible abundances or absence.

Conclusions

Our findings indicate that *D. oculata* and *O. davisae* have become well established in the Israeli Levantine Sea and have successfully adapted to different coastal environments, becoming a significant part of the mesozooplankton community across the EMS. Information on the ecosystem status before the introduction of *D. oculata* and *O. davisae*, including the abundance of predators, prey, and competitors, is unavailable. Nevertheless, we can hypothesize that, with the acceleration of warming in this region, native species will be more susceptible to the detrimental effects of warming, as has been shown for various benthic species (Rilov, 2016). The prolonged warming trend of 1.2 °C per decade in the EMS (Ozer *et al.* 2017) has facilitated its tropicalization, promoting the establishment and spread of tropical non-native copepod species such as *D. oculata* in the Levantine Basin. Similarly, the high ecological plasticity of *O. davisae* has made this cyclopoid species one of the most successful invasive copepods in the Mediterranean Sea. Ecophysiological studies of the recently introduced *D. oculata* are needed to understand its invasion success in the EMS. We further stress the importance of monitoring non-native cyclopoid species to understand their functionality in colonized areas.

Acknowledgements

This study was supported by the National Israeli monitoring program of the Mediterranean Sea and the Open Collaborative Research Fund of Hong Kong Brach of Southern Marine Science and Engineering Guangdong Laboratory (No. 20190008) to T.G.-H. and D.M. *Oithona davisae* specimens from the Aegean Sea were collected for molecular analysis during the project “Integrated Marine Pollution Monitoring 2017-2019 Programme” carried out by Ministry of Environment and Urbanization/ General Directorate of EIA, Permit and Inspection/Department of Laboratory, Measurement and coordinated by TUBITAK-MRC ECPI, Grant/Award Number: ctue.17.2113. We thank the Sea Team of the Israeli Oceanographic and Limnological Research for assistance in sampling. We also thank the reviewers and the editor Dr. Maria Grazia Mazzocchi for the constructive comments, which substantially helped us to improve the manuscript.

References

- Abdel-Rahman, N.S., 2005. The immigration progress of planktonic Copepoda across the Suez Canal, Egypt. *Egyptian Journal of Aquatic Biology and Fisheries*, 9 (3), 59-82.
- Almeda, R., Augustin, C.B., Alcaraz, M., Calbet, A., Saiz, E., 2010. Feeding rates and gross growth efficiencies of larval developmental stages of *Oithona davisae* (Copepoda, Cyclopoida). *Journal of Experimental Marine Biology and Ecology*, 387 (1-2), 24-35.
- Altukhov, D.A., Gubanov, A.D., Mukhanov, V.S., 2014. New invasive copepod *Oithona davisae* Ferrari and Orsi, 1984: Seasonal dynamics in Sevastopol Bay and expansion along the Black Sea coasts. *Marine Ecology*, 35 (Suppl), 28-34.
- Andrews, K.R., Norton, E.L., Fernandez-Silva, I., Portner, E., Goetze, E., 2014. Multilocus evidence for globally distributed cryptic species and distinct populations across ocean gyres in a mesopelagic copepod. *Molecular Ecology*, 23, 5462-5479.
- Ambler, J.W., Ferrari, F.D., Fornshell, J.A., 1991. Population structure and swarm formation of the cyclopoid copepod *Dioithona oculata* near mangrove cays. *Journal of Plankton Research*, 13 (6), 1257-1272.
- Ambler, J.W., 2002. Zooplankton swarms: Characteristics, proximal cues and proposed advantages. *Hydrobiologia*, 480, 155-164.
- Armon, R.H., Zenetos, A., 2015. Environmental indicators. *Environmental Indicators*, 1-1068.
- Bianchi, C.N., Morri, C., 2003. Global sea warming and “tropicalization” of the Mediterranean Sea: biogeographic and ecological aspects. *Biogeographia*, 24 (1), 319-327.
- Boxshall, G.A., Halsey, S.H., 2004. *An introduction to copepod diversity*. Cold Spring Harbor Laboratory Press, London, 234 pp.
- Bucklin, A., Ortman, B.D., Jennings, R.M., Nigro, L.M., Sweetman, C.J. *et al.*, 2010. A “Rosetta Stone” for metazoan zooplankton: DNA barcode analysis of species diversity of the Sargasso Sea (Northwest Atlantic Ocean). *Deep Sea Research Part II. Topical Studies in Oceanography*, 57 (24-

- 26), 2234-2247.
- Buskey, E.J., 1998. Energetic costs of swarming behavior for the copepod *Dioithona oculata*. *Marine Biology*, 130 (3), 425-431.
- Buskey, E.J., Hyatt, C.J., Speckmann, C.L., 2004. Trophic interactions within the planktonic food web in mangrove channels of Twin Cays, Belize, Central America. *Atoll Research Bulletin*, 1-24.
- Bradford-Grieve, J.M., Markhaseva, E.L., Rocha, C.E.F., Abi-ahy, B., 1999. Copepoda. p. 872-977. In: *South Atlantic Zooplankton*. Boltovskoy, D. (Eds). Backhuys Publishers, Netherlands.
- Castellani, C., Irigoien, X., Harris, R.P., Holliday, N.P., 2007. Regional and temporal variation of *Oithona* spp. biomass, stage structure and productivity in the Irminger Sea, North Atlantic. *Journal of Plankton Research*, 29 (12), 1051-1070.
- Checkley, D.M., Uye, S., Dagg, M.J., Mullin, M.M., Omori, M. *et al.*, 1992. Diel variation of the zooplankton and its environment at neritic stations in the Inland sea of Japan and the north-west Gulf of Mexico. *Journal of Plankton Research*, 14 (1), 1-40.
- Chen, G., Hare, M.P., 2011. Cryptic diversity and comparative phylogeography of the estuarine copepod *Acartia tonsa* on the US Atlantic coast. *Molecular Ecology*, 20 (11), 2425-2441.
- Choi, K.H., Kimmerer, W., Smith, G., Ruiz, G.M., Lion, K., 2005. Postex change zooplankton in ballast water of ships entering the San Francisco Estuary. *Journal of Plankton Research*, 27, 707-714.
- Çınar, M.E., Bilecenoglu, M., Ozturk, B., Katagan, T., Aysel, V., 2005. Alien species on the coasts of Turkey. *Mediterranean Marine Science*, 6 (2), 119-146.
- Cornils, A., Held, C., 2014. Evidence of cryptic and pseudocryptic speciation in the *Paracalanus parvus* species complex (Crustacea, Copepoda, Calanoida). *Frontiers in Zoology*, 11 (1), 19.
- Cornils, A., Wend-Heckmann, B., 2015. First report of the planktonic copepod *Oithona davisae* in the northern Wadden Sea (North Sea): Evidence for recent invasion? *Helgoland Marine Research*, 69 (2), 243-248.
- Cornils, A., Wend-Heckmann, B., Held, C., 2017. Global phylogeography of *Oithona similis* sl (Crustacea, Copepoda, Oithonidae)—A cosmopolitan plankton species or a complex of cryptic lineages? *Molecular Phylogenetics and Evolution*, 107, 473-485.
- Dahms, H.U., Tseng, L.C., Hwang, J.S., 2015. Biogeographic distribution of the cyclopoid copepod genus *Oithona* - from mesoscales to global scales. *Journal of Experimental Marine Biology and Ecology*, 467, 26-32.
- Doğan, G., Isinibilir, M., 2016. First report of a new invasive species *Oithona davisae* Ferrari and Orsi, 1984 (Copepoda: Cyclopoida) in the Sea of Marmara. *Turkish Journal of Fisheries and Aquatic Sciences*, 16 (2), 469-473.
- Dragicevic, B., Anadoli, O., Angel, D., Benabdi, M., Bitar, G. *et al.*, 2019. New Mediterranean Biodiversity Records (December 2019). *Mediterranean Marine Science*, 20 (3), 645-656.
- Ferrari, F.D., Orsi, J., 1984. *Oithona Davisae*, New Species, and *Limnoithona Sinensis* (Burckhardt, 1912) (Copepoda: Oithonidae) From the Sacramento-san Joaquin Estuary, California. *Journal of Crustacean Biology*, 4 (1), 106-126.
- Gubanova, A., Altukhov, D., 2007. Establishment of *Oithona brevicornis* Giesbrecht, 1892 (Copepoda: Cyclopoida) in the Black Sea. *Aquatic Invasions*, 2, 407-410.
- Hirakawa, K., 1988. New records of the North Pacific coastal planktonic copepods, *Acartia omorii* (Acartiidae) and *Oithona davisae* (Oithoniidae) from South Chile. *Bulletin of Marine Sciences*, 42, 337-339.
- Hall, T.A., 1999. BioEdit: A User-Friendly Biological Sequence Alignment Editor and Analysis Program for Windows 95/98/NT. *Nucleic Acids Symposium Series*, 41, 95-98.
- Hammer, W.M., Carleton, J.H., 1979. Copepod swarms: attributes and role in coral reef ecosystems. *Limnology and Oceanography*, 24 (1), 1-14.
- Henriksen, C.I., Saiz, E., Calbet, A., Hansen, B.W., 2007. Feeding activity and swimming patterns of *Acartia grani* and *Oithona davisae* nauplii in the presence of motile and non-motile prey. *Marine Ecology Progress Series*, 331, 119-129.
- Hirota, R., 1990. Microdistribution of the marine copepod *Oithona davisae* in the shallow waters of Ariake-kai mud flats, Japan. *Marine Biology*, 105, 307-312.
- Hirota, R., Tanaka, Y., 1985. High abundance of *Oithona davisae* (Copepoda: Cyclopoida) in the shallow waters adjacent to the mud flats in Ariake kai, western Kyushu. *Bulletin of the Plankton Society of Japan*, 32, 169-170.
- Hsiao, Y.H., Dahms, H.U., Hwang, J.S., 2013. Ecology of swarming in the planktonic copepod *Dioithona* sp. (Crustacea: Copepoda). *Journal of Natural History*, 47 (5-12), 739-751.
- Hsu, P.K., Lo, W.T., Shih, C., 2008. The coupling of copepod assemblages and hydrography in a eutrophic lagoon in Taiwan: seasonal and spatial variations. *Zoological Studies*, 47 (2), 172-184.
- Hubareva, E., Svetlichny, L., 2013. Salinity and temperature tolerance of alien copepods *Acartia tonsa* and *Oithona davisae* in the Black Sea. *Rapport de la Commission Internationale pour l'Exploration scientifique de la Mer Méditerranée*, 40, 742.
- Hwang, J.S., Kumar, R., Dahms, H.U., Tseng, L.C., Chen, Q.C., 2010. Interannual, seasonal, and diurnal variations in vertical and horizontal distribution patterns of 6 *Oithona* spp. (Copepoda: Cyclopoida) in the South China Sea. *Zoological Studies*, 49 (2), 220-229.
- İşinibilir, M., Doğan, O., 2019. Zooplankton Biodiversity in the Golden Horn Estuary after the Opening of the Water Channel from the Strait of Istanbul, Turkey. *Turkish Journal of Fisheries Sciences*, 20 (2), 147-158.
- Jungbluth, M.J., Lenz, P.H., 2013. Copepod diversity in a subtropical bay based on a fragment of the mitochondrial COI gene. *Journal of plankton research*, 35 (3), 630-643.
- Khodami, S., Mercado-Salas, N.F., Tang, D., Arbizu, P.M. 2019. Molecular evidence for the retention of the Thaumapsyllidae in the order Cyclopoida (Copepoda) and establishment of four suborders and two families within the Cyclopoida. *Molecular Phylogenetics and Evolution*, 138, 43-52.
- Katsanevakis, S., Coll, M., Piroddi, C., Steenbeek, J., Lasram, F.B.R. *et al.*, 2014. Invading the Mediterranean Sea: Biodiversity patterns shaped by human activities. *Frontiers in Marine Science*, 1, 1-11.
- Khanaychenko, A., Mukhanov, V., Aganesova, L., Besiktepe,

- S., Gavrilova, N., 2018. Grazing and feeding selectivity of *Oithona davisae* in the Black Sea: Importance of cryptophytes. *Turkish Journal of Fisheries and Aquatic Sciences*, 18 (8), 937-949.
- Kimor, B., Wood, E.J.F., 1975. A plankton study in the eastern Mediterranean Sea. *Marine Biology*, 29 (4), 321-333.
- Kiefer F., 1935. Zur Kenntnis der Oithonidae. *Zoologischer Anzeiger*, 112, 322-327.
- Kjørboe, T., 2007. Mate finding, mating, and population dynamics in a planktonic copepod *Oithona davisae*: there are too few males. *Limnology and Oceanography*, 52 (4), 1511-1522.
- Kjørboe, T., 2011. How zooplankton feed: mechanisms, traits and trade-offs. *Biological Reviews*, 86 (2), 311-339.
- Kumar, S., Stecher, G., Li, M., Knyaz, C., Tamura, K., 2018. MEGA X: molecular evolutionary genetics analysis across computing platforms. *Molecular Biology and Evolution*, 35 (6), 1547-1549.
- Lasram, F.B.R., Tomasini, J.A., Guilhaumon, F., Romdhane, M.S., Do Chi, T. *et al.*, 2008. Ecological correlates of dispersal success of Lessepsian fishes. *Marine Ecology Progress Series*, 363, 273-286.
- Lo, W.T., Chung, C.L., Shih, C.T., 2004. Seasonal distribution of copepods in Tapong Bay, southwestern Taiwan. *Zoological Studies*, 43 (2), 464-474.
- Mannino, A.M., Balistreri, P., Deidun, A., 2017. The Marine Biodiversity of the Mediterranean Sea in a Changing Climate: The Impact of Biological Invasions. p. 102-127. In: *Mediterranean Identities - Environment, Society, Culture*. Fuerst-Bjelis, B. (Eds). SPi Global, Croatia.
- Mazzocchi, M.G., Siokou, I., Tirelli, V., Bandelj, V., Fernandez de Puelles, M.L. *et al.*, 2014. Regional and seasonal characteristics of epipelagic mesozooplankton in the Mediterranean Sea based on an artificial neural network analysis. *Journal of Marine Systems*, 135, 64-80.
- Motoda, S., 1959. Devices of simple plankton apparatus. *Memoirs of the Faculty of Fisheries Hokkaido University*, 7 (1-2), 73-94.
- Mihneva, V., Stefanova, K., 2013. The non-native copepod *Oithona davisae* (Ferrari FD and Orsi, 1984) in the Western Black Sea: seasonal and annual abundance variability. *Bio-Invasions Record*, 2, 119-124.
- Nishida, S., 1985. Taxonomy and distribution of the family Oithonidae (Copepoda, Cyclopoida) in the Pacific and Indian Oceans. *Bulletin of the Ocean Research Institute, University of Tokyo*, 20, 1-167.
- Occhipinti-Ambrogi, A., Galil, B., 2010. Marine alien species as an aspect of global change. *Advances in Oceanography and Limnology*, 1 (1), 199-218.
- Oksanen, J., Blanchet, F.G., Kindt, R., Friendly, M., Legendre, P. *et al.*, 2013). Vegan: community ecology package. Available <http://cran.r-project.org/web/packages/vegan/index.Htm>. (Accessed June 15, 2021).
- Ozer, T., Gertman, I., Kress, N., Silverman, J., Herut, B., 2017. Interannual thermohaline (1979–2014) and nutrient (2002–2014) dynamics in the Levantine surface and intermediate water masses, SE Mediterranean Sea. *Global and Planetary Change*, 151, 60-67.
- Pansera, M., Camatti, E., Schroeder, A., Zagami, G., Bergamasco, A., 2021. The non-indigenous *Oithona davisae* in a Mediterranean transitional environment: coexistence patterns with competing species. *Scientific Reports*, 11 (1), 1-14.
- Raveh, O., David, N., Rilov, G., Rahav, E., 2015. The temporal dynamics of coastal phytoplankton and bacterioplankton in the Eastern Mediterranean Sea. *PLoS ONE*, 10 (10), e0140690.
- Razouls C., Desreumaux N., Kouwenberg J., de Bovée F., 2005-2021. Biodiversity of Marine Planktonic Copepods (morphology, geographical distribution and biological data). Sorbonne University, CNRS. Available at <http://copepodes.obs-banyuls.fr/en> (Accessed June 29, 2020).
- Rezai, H., Yusoff, F.M., Arshad, A., Kawamura, A., Nishida, S. *et al.*, 2004. Spatial and temporal distribution of copepods in the Straits of Malacca. *Zoological Studies*, 43 (2), 486-497.
- Riccardi, N., 2010. Selectivity of plankton nets over mesozooplankton taxa: implications for abundance, biomass and diversity estimation. *Journal of Limnology*, 69 (2), 287-296.
- Rilov, G., 2016. Multi-species collapses at the warm edge of a warming sea. *Scientific Reports*, 6 (1), 1-14.
- Robinson, A.R., Malanotte-Rizzoli, P., Hecht, A., Michelato, A., Roether, W. *et al.*, 1992. General circulation of the Eastern Mediterranean. *Earth-Science Reviews*, 32 (4), 285-309.
- Sabia, L., Zagami, G., Mazzocchi, M.G., Zambianchi, E., Uttieri, M., 2015. Spreading factors of a globally invading coastal copepod. *Mediterranean Marine Science*, 16 (2), 460-471.
- Saiz, E., Calbet, A., Broglio, E. 2003. Effects of small-scale turbulence on copepods: The case of *Oithona davisae*. *Limnology and Oceanography*, 48 (3), 1304-1311.
- Santhosh, B., Anil, M.K., Muhammed Anzeer, F., Aneesh, K. S., Mijo, V. (Eds.), 2018. Culture techniques of marine copepods. ICAR-Central Marine Fisheries Research Institute, Kochi, Kerala, India, 144pp.
- Selifonova, Z.P., 2009. *Oithona brevicornis* Giesbrecht (Copepoda, Cyclopoida) in harborages of the northeastern part of the Black Sea shelf. *Inland Water Biology*, 2 (1), 30-32.
- Shiganova, T., Stupnikova, A., Stefanova, K., 2015. Genetic analyses of non-native species *Oithona davisae* Ferrari FD & Orsi, 1984 in the Black Sea. *BioInvasions Records*, 4 (2), 91-95.
- Stupnikova, A.N., Molodtsova, T.N., Mugue, N.S., Neretina, T.V., 2013. Genetic variability of the *Metridia lucens* complex (Copepoda) in the Southern Ocean. *Journal of Marine Systems*, 128, 175184.
- Svetlichny, L., Hubareva, E., 2014. Salinity tolerance of alien copepods *Acartia tonsa* and *Oithona davisae* in the Black Sea. *Journal of Experimental Marine Biology and Ecology*, 461, 201-208.
- Svetlichny, L., Hubareva, E., Khanaychenko, A., Gubanov, A., Altukhov, D. *et al.*, 2016. Adaptive strategy of thermophilic *Oithona davisae* in the cold black sea environment. *Turkish Journal of Fisheries and Aquatic Sciences*, 16 (1), 77-90.
- Svetlichny, L., Hubareva, E., İşinibilir, M., 2018. Population dynamics of the copepod invader *Oithona davisae* in the Black Sea. *Turkish Journal of Zoology*, 42, 684-693.
- Svetlichny, L., Hubareva, E., Uttieri, M., 2020. Ecophysiological and behavioural responses to salinity and temperature stress in cyclopoid copepod *Oithona davisae* with com-

- ments on gender differences. *Mediterranean Marine Science*, 22 (1), 89-101.
- Temnykh, A., Nishida, S., 2012. New record of the planktonic copepod *Oithona davisae* Ferrari and Orsi, 1984 in the Black Sea with notes on the identity of *Oithona brevicornis*. *Aquatic Invasions*, 7 (3), 425-431.
- Terbiyik Kurt, T., 2018. Contribution and acclimatization of the swarming tropical copepod *Dioithona oculata* (Farran, 1913) in a mediterranean coastal ecosystem. *Turkish Journal of Zoology*, 42 (5), 567-577.
- Terbiyik Kurt, T., Beşiktepe, Ş., 2019. First distribution record of the invasive copepod *Oithona davisae* Ferrari and Orsi, 1984, in the coastal waters of the Aegean Sea. *Marine Ecology*, 40 (3), e12548.
- Terbiyik Kurt, T., 2020a. The distribution of indopasific *Dioithona oculata* in southern coastal waters of Turkey. *Aquatic Research*, 3(4), 197-207.
- Terbiyik Kurt, T., 2020b. The expanded distribution of the invasive alien copepod *Oithona davisae* in the Mediterranean Sea: review. p. 215. In: 7th International Conference on Engineering & Natural Sciences. May 8-10 2020. ISPEC, Izmir, Turkey.
- Turner, J.T., 2004. The importance of small planktonic copepods and their roles in pelagic marine food webs. *Zoological Studies*, 43 (2), 255-266.
- Uriarte, I., Villate, F., Iriarte, A., 2016. Zooplankton recolonization of the inner estuary of Bilbao: influence of pollution abatement, climate and non-indigenous species. *Journal of Plankton Research*, 38 (3), 718-731.
- Üstün, F., Terbiyik Kurt, T., 2016. First Report of the Occurrence of *Oithona Davisae* Ferrari FD & Orsi, 1984 (Copepoda: Oithonidae) in the Southern Black Sea, Turkey. *Turkish Journal of Fisheries and Aquatic Sciences*, 16 (2), 413-420.
- Uye, S., Sano, K., 1995. Seasonal reproductive biology of the small cyclopoid copepod *Oithona davisae* in a temperate eutrophic inlet. *Marine Ecology Progress Series*, 118 (1-3), 121-128.
- Uye, S.I., Sano, K., 1998. Seasonal variations in biomass, growth rate and production rate of the small cyclopoid copepod *Oithona davisae* in a temperate eutrophic inlet. *Marine Ecology Progress Series*, 163, 37-44.
- Vervoort, W., 1964. Free-living Copepoda from Ifaluk Atoll in the Caroline Islands with notes on related species. *Bulletin of the United States National Museum*, 23, 1-431.
- Vidjak, O., Bojanić, N., de Olazabal, A., Benzi, M., Brautović, I. et al., 2019. Zooplankton in Adriatic port environments: Indigenous communities and non-indigenous species. *Marine Pollution Bulletin*, 147, 133-149.
- Wellershaus, S., 1969. On the taxonomy of planktonic Copepoda in the Cochin Backwater (a South Indian Estuary). *Veroff Inst Meeresforsch Bremerhaven*, 11, 245-286.
- Yıldız, İ., Feyzioğlu, A.M., Beşiktepe, S., 2016. First observation and seasonal dynamics of the new invasive planktonic copepod *Oithona davisae* Ferrari and Orsi, 1984 along the southern Black Sea (Anatolian Coast). *Journal of Natural History*, 51, 127-139.
- Zagami, G., Brugnano, C., Granata, A., Guglielmo, L., Minutoli, R. et al., 2018. Biogeographical distribution and ecology of the planktonic copepod *Oithona davisae*: Rapid invasion in Lakes Faro and Ganzirri (Central Mediterranean Sea). p. 59-82. In: *Trends in Copepod Studies - Distribution, Biology and Ecology*. Uttieri, M. (Eds). Nova Science Publishers, New York.
- Zagorodnyaya, Y.A., 2002. *Oithona brevicornis* in Sevastopol Bay: Is it a single event or a new invader in the Black Sea fauna? *Ecologiya Morya*, 61, 43.
- Zakaria, H.Y., 2015. Article Review: Lessepsian migration of zooplankton through Suez Canal and its impact on ecological system. *Egyptian Journal of Aquatic Research*, 41 (2), 129-144.
- Zamora-Terol, S., Saiz, E., 2013. Effects of food concentration on egg production and feeding rates of the cyclopoid copepod *Oithona davisae*. *Limnology and Oceanography*, 58 (1), 376-387.
- Zenetos, A., Gofas, S., Verlaque, M., Çinar, M.E., García Raso, J. G. et al., 2010. Alien species in the Mediterranean Sea by 2010. A contribution to the application of European Union's Marine Strategy Framework Directive (MSFD). Part I. Spatial distribution. *Mediterranean Marine Science*, 11 (2), 381-493.
- Zenetos, A., Gofas, S., Morri, C., Rosso, A., Violanti, D. et al., 2012. Alien species in the Mediterranean Sea by 2012. A contribution to the application of European Union's Marine Strategy Framework Directive (MSFD). Part 2. Introduction trends and pathways. *Mediterranean Marine Science*, 13 (2), 328-352.
- Zenetos, A., Karachle, P.K., Corsini-Foka, M., Gerovasileiou, V., Simboura, N. et al., 2020. Is the trend in new introductions of marine non-indigenous species a reliable criterion for assessing good environmental status? The case study of Greece. *Mediterranean Marine Science*, 21 (3), 775-793.
- Zervoudaki, S., Christou, E.D., Nielsen, T.G., Siokou-Frangou, I., Assimakopoulou, G. et al., 2007. The importance of small-sized copepods in a frontal area of the Aegean Sea. *Journal of Plankton Research*, 29 (4), 317-338.

Supplementary data

The following supplementary information is available online for the article:

Video S1. *Dioithona oculata* external morphology. Video was made using Olympus SC180 camera mounted on Olympus SZX16 stereomicroscope (Olympus, Japan).